



UNIVERSITÀ DI PARMA

ARCHIVIO DELLA RICERCA

University of Parma Research Repository

Laminar Origin of Corticostriatal Projections to the Motor Putamen in the Macaque Brain

This is the peer reviewed version of the following article:

Original

Laminar Origin of Corticostriatal Projections to the Motor Putamen in the Macaque Brain / Borra, Elena; Rizzo, Marianna; Gerbella, Marzio; Rozzi, Stefano; Luppino, Giuseppe. - In: THE JOURNAL OF NEUROSCIENCE. - ISSN 1529-2401. - 41:(2021), pp. 1455-1469. [10.1523/JNEUROSCI.1475-20.2020]

Availability:

This version is available at: 11381/2891270 since: 2022-01-10T11:25:46Z

Publisher:

Society for Neuroscience

Published

DOI:10.1523/JNEUROSCI.1475-20.2020

Terms of use:

Anyone can freely access the full text of works made available as "Open Access". Works made available

Publisher copyright

note finali coverpage

(Article begins on next page)

12 August 2025

Research Articles: Systems/Circuits

Laminar origin of corticostriatal projections to the motor putamen in the macaque brain

<https://doi.org/10.1523/JNEUROSCI.1475-20.2020>

Cite as: J. Neurosci 2020; 10.1523/JNEUROSCI.1475-20.2020

Received: 9 June 2020

Revised: 1 December 2020

Accepted: 4 December 2020

This Early Release article has been peer-reviewed and accepted, but has not been through the composition and copyediting processes. The final version may differ slightly in style or formatting and will contain links to any extended data.

Alerts: Sign up at www.jneurosci.org/alerts to receive customized email alerts when the fully formatted version of this article is published.

1 **Laminar origin of corticostriatal projections to the motor putamen in the macaque brain**

2 Elena Borra, Marianna Rizzo, Marzio Gerbella, Stefano Rozzi, Giuseppe Luppino

3 Università di Parma, Dipartimento di Medicina e Chirurgia, Via Volturno 39E, 43125 Parma, Italy

4 **Corresponding authors:** Elena Borra. E mail: elena.borra@unipr.it

5

6 **Abbreviated title:** Laminar origin of corticostriatal projections

7 **Keywords:** Basal ganglia; Striatum; Motor control; Striatal input channels; Layer VI; Primates

8

9 **Number of figures and tables:** 10 Figures, 3 Tables

10 **Number of pages:** 33

11 **Number of words:** in abstract (240), introduction (597), discussion (1560)

12

13 **Conflict of interest:** The authors declare no competing financial interests.

14 **Acknowledgements:** This research has financially been supported by the Programme “FIL-Quota
15 Incentivante” of University of Parma and co-sponsored by Fondazione Cariparma and by Ministero
16 dell’Istruzione, dell’Università e della Ricerca (Grant number: PRIN 2017, n°2017KZNZLN_002).

17 The 3D reconstruction software was developed by CRS4, Pula, Cagliari, Italy.

18

19 **ABSTRACT**

20 In the macaque brain, projections from distant, interconnected cortical areas converge in specific
21 zones of the striatum. For example, specific zones of the motor putamen are targets of projections
22 from frontal motor, inferior parietal and ventrolateral prefrontal hand-related areas and thus are
23 integral part of the so-called “lateral grasping network”. In the present study, we analyzed the
24 laminar distribution of corticostriatal neurons projecting to different parts of the motor putamen.
25 Retrograde neural tracers were injected in different parts of the putamen in 3 *Macaca mulatta* (one
26 male) and the laminar distribution of the labeled corticostriatal neurons was analyzed quantitatively.
27 In frontal motor areas and frontal operculum, where most labeled cells were located, almost
28 everywhere the proportion of corticostriatal labeled neurons in layers III and/or VI was comparable
29 or even stronger than in layer V. Furthermore, within these regions, the laminar distribution pattern
30 of corticostriatal labeled neurons largely varied independently from their density and from the
31 projecting area/sector, but likely according to the target striatal zone. Accordingly, the present data
32 show that cortical areas may project in different ways to different striatal zones, which can be
33 targets of specific combinations of signals originating from the various cortical layers of the areas
34 of a given network. These observations extend current models of corticostriatal interactions,
35 suggesting more complex modes of information processing in the basal ganglia for different motor
36 and non-motor functions and opening new questions on the architecture of the corticostriatal
37 circuitry.

38

39 **SIGNIFICANT STATEMENT**

40 Projections from the ipsilateral cerebral cortex are the major source of input to the striatum.
41 Previous studies have provided evidence for distinct zones of the putamen specified by converging
42 projections from specific sets of interconnected cortical areas. The present study shows that the
43 distribution of corticostriatal neurons in the various layers of the primary motor and premotor areas
44 varies depending on the target striatal zone. Accordingly, different striatal zones collect specific
45 combinations of signals from the various cortical layers of their input areas, possibly differing in
46 terms of coding, timing and direction of information flow (e.g., feed-forward, or feed-back).

47

48 **INTRODUCTION**

49 Projections from the ipsilateral cerebral cortex are the major source of input to the striatum, the
50 main input station of the basal ganglia (cortico-basal ganglia-thalamo-cortical) loop.

51 According to early models, different striatal territories are a target of specific cortical regions
52 and in turn are at the origin of largely segregated basal ganglia-thalamo-cortical loops (Alexander et
53 al., 1986). Subsequent studies confirmed this view, but also showed up a finer modular organization
54 in which each main loop consists of several largely segregated closed subloops. In this view, each
55 subloop originates from, and projects to, individual cortical areas or limited sets of functionally
56 related areas and involves distinct, relatively restricted striatal zones, which have been referred to as
57 “input channels” (Strick et al. 1995; Middleton and Strick 2000). The various subloops, because of
58 their differential cortical origin and termination, could be functionally distinct and their definition is
59 thus essential for understanding the mode of information processing in the basal ganglia for
60 different motor and non-motor functions.

61 In this context, one important aspect is the definition of the way in which cortical areas or
62 sectors contribute to the projections to a specific striatal zone in terms of laminar origin of their
63 projections. Based on studies carried out in different animal species, it is largely agreed that
64 corticostriatal (CSt) neurons are typically located mostly in layer V and, in some cases, layer III of
65 most cortical areas (see Gerfen and Bolam, 2010). In the macaque brain, based on retrograde tracer
66 injections in the caudate, the contribution of layer III in the temporal and prefrontal cortex was
67 found to be correlated with the density of CSt labeled cells (Arikuni and Kubota, 1986; Saint-cyr et
68 al., 1990). Recently, this view has been seriously challenged by data of Griggs et al. (2017), based
69 on retrograde tracer injections in the head or the tail of the macaque caudate showing that: i) in the
70 temporal cortex, laminar patterns of CSt projections from a given cortical sector markedly differ
71 according to the striatal target; and ii) layer VI can heavily contribute to the projections to specific
72 striatal targets.

73 Accordingly, laminar patterns of CSt projections could be more complex than previously
74 considered and could represent an important variable to evaluate in defining the possible
75 contribution of cortical areas to the projections to a specific putaminal zone.

76 In the present study, we addressed this issue focusing on the macaque CSt projections to the
77 so-called “motor putamen”, i.e., that part of the putamen that is a target of massive projections from
78 the various subdivisions of the primary motor and premotor areas (frontal motor areas). Previous
79 studies have provided evidence for converging projections from different sets of frontal and
80 cingulate motor areas in different parts of the motor putamen (Takada et al., 1998; Nambu, 2011).
81 Recent data (Gerbella et al., 2016) showing that projections from hand-related ventral premotor,
82 inferior parietal, and ventrolateral prefrontal areas forming the “lateral grasping network” (Borra et
83 al., 2017) overlap in two distinct putaminal zones, suggested an even more complex pattern of
84 converging input for parallel processing of different aspects of motor and non-motor functions.

85 Specifically, based on retrograde tracer injections in different parts of the motor putamen, we
86 have analyzed the laminar distribution of the labeled CSt neurons. Main aims were to: i) quantify
87 the contribution of the different cortical layers to the projections to a given relatively restricted
88 putaminal zone; ii) see whether these contributions vary within the various labeled cortical regions;
89 iii) assess whether possible differences in laminar distribution patterns are related to the labeled
90 cells density, the cortical area, or the target putaminal zone.

91

92

93 **METHODS**94 **Subjects, surgical procedures, and selection of the injection sites**

95 The experiments were carried out in three *Macaca mulatta* (Cases 61, 71, and 75, one male), in
96 which retrograde neural tracers were injected in the putamen. Animal handling as well as surgical
97 and experimental procedures complied with the European law on the humane care and use of
98 laboratory animals (directives 86/609/EEC, 2003/65/CE, and 2010/63/EU) and Italian laws in force
99 regarding the care and use of laboratory animals (D.L. 116/92 and 26/2014), and were periodically
100 approved by the Veterinarian Animal Care and Use Committee of the University of Parma and
101 authorized by the Italian Ministry of Health.

102 Before the injection of neural tracers, we obtained scans of each brain using magnetic
103 resonance imaging (MRI; Cases 71 and 75: 7 T General Electric, Boston, MA; Case 61: 0.22 T
104 Paramed Medical Systems, Genova, Italy) to calculate the stereotaxic coordinates of the putaminal
105 target regions and the best trajectory of the needle to reach it.

106 Under general anesthesia (Cases 61 and 71: Zoletil®, initial dose 20 mg/kg, i.m.,
107 supplemental 5–7 mg/kg/hr, i.m., or Ketamine, 5 mg/kg i.m. and Medetomidine, 0.08–0.1 mg/kg
108 i.m.; Case 75: induction with Ketamine 10 mg/kg, i.m. followed by intubation, isoflurane 1.5–2%)
109 and aseptic conditions, each animal was placed in a stereotaxic apparatus and an incision was made
110 in the scalp. The skull was trephined to remove the bone and the dura was opened to expose a small
111 cortical region. After tracer injections, the dural flap was sutured, the bone was replaced, and the
112 superficial tissues were sutured in layers. During surgery, hydration was maintained with saline, and
113 heart rate, blood pressure, respiratory depth, and body temperature were continuously monitored.
114 Upon recovery from anesthesia, the animals were returned to their home cages and closely
115 observed. Dexamethasone (0.5 mg/kg, i.m.) and prophylactic broad-spectrum antibiotics (e.g.,
116 Ceftriaxone 80 mg/kg, i.m.) were administered pre- and postoperatively, as were analgesics (e.g.,
117 Ketoprofen 5 mg/kg i.m.).

118

119 **Tracer injections and histological procedures**

120 Based on stereotaxic coordinates, the neural tracers Fast Blue (FB, 3% in distilled water, Dr Illing
121 Plastics GmbH, Breuberg, Germany) and Cholera Toxin B subunit, conjugated with Alexa 488
122 (CTB green, CTBg; 1% in 0.01 M phosphate-buffered saline at pH 7.4, Molecular Probes, Thermo
123 Fisher Scientific, Waltham, MA) were slowly pressure-injected through a stainless steel 31 gauge
124 beveled needle attached through a polyethylene tube to a Hamilton syringe (Hamilton Company,
125 Reno NV). In Cases 71 and 75, the injection needle was lowered to the putamen within a guiding
126 tube, to avoid tracer spillover in the white matter. Table 1 summarizes the locations of the
127 injections, the injected tracers, and the amounts injected.

128 After appropriate survival periods following the injections (28 days for FB and 14 days for
129 CTBg), each animal was deeply anesthetized with an overdose of sodium thiopental and perfused
130 through the left cardiac ventricle consecutively with saline (about 2 L in 10 min), 3.5%
131 formaldehyde (5 L in 30 min), and 5% glycerol (3 L in 20 min), all prepared in 0.1 M phosphate
132 buffer, pH 7.4. Each brain was then blocked coronally on a stereotaxic apparatus, removed from the
133 skull, photographed, and placed in 10% buffered glycerol for 3 days and 20% buffered glycerol for
134 4 days. In Case 75, the right inferotemporal cortex was removed for other experimental purposes.
135 Finally, each brain was cut frozen into coronal sections of 60- μm (Cases 61 and 75) or 50- μm (Case
136 71) thickness.

137 In all cases, sections spaced 300 μm apart - that is one section in each repeating series of 5 in
138 Cases 61 and 75 and one in series of 6 in Case 71- were mounted, air-dried, and quickly
139 coverslipped for fluorescence microscopy. Another series of each fifth section (sixth in Case 71)
140 was processed for visualizing CTBg with immunohistochemistry. Specifically, endogenous
141 peroxidase activity was eliminated by incubation in a solution of 0.6% hydrogen peroxide and 80%
142 methanol for 15 min at room temperature. The sections were then incubated for 72 h at 4°C in a
143 primary antibody solution of rabbit anti-Alexa 488 (1:15000, Thermo Fisher Scientific; RRID:
144 AB_221544) in 0.5% Triton, 5% normal goat serum in PBS, and for 1 h in biotinylated secondary

145 antibody (1:200, Vector Laboratories, Burlingame, CA) in 0.3% Triton, 5% normal goat serum in
146 PBS. Finally, CTBg labeling was visualized using the Vectastain ABC kit and then a solution of
147 3,3'-diaminobenzidine (50 mg/100ml; DAB, Sigma-Aldrich, St. Louis, MO), 0.01% hydrogen
148 peroxide, 0,02% cobalt chloride and 0,03% nickel ammonium sulfate in 0.1M phosphate buffer. In
149 Case 75, a subset of sections spaced 1200 μ m immunostained for CTBg, were then incubated
150 overnight at room temperature in a primary antibody solution of rabbit anti-NeuN (1:5000, Cell
151 Signaling Technology, Danvers, MA; RRID: AB_2630395) in 0.3% Triton, 5% normal goat serum
152 in PBS, and for 1 h in biotinylated secondary antibody (1:100, Vector Laboratories) in 0.3% Triton,
153 5% normal goat serum in PBS. Finally, NeuN positive cells were visualized using the Vectastain
154 ABC kit and DAB as a chromogen. With this protocol, in the same tissue sections CTBg labeling
155 was stained black and NeuN positive cells were stained brown. In Case 75, an additional subset of
156 sections spaced 1200 μ m through the frontal lobe, were incubated in a primary antibody solution of
157 anti-Alexa 488 and in a biotinylated secondary antibody solution as described above, followed by
158 incubation for 1 h in a solution of streptavidin Alexa 488 – conjugated (1:500, Invitrogen) in PBS
159 with 0.5% Triton. The same sections were then incubated overnight at room temperature in a
160 primary antibody solution of mouse monoclonal SMI-32 (1:5000; Covance, Princeton, NJ; RRID:
161 AB_2315331), in PBS with 0.5% Triton and 2% normal goat serum, and for 1 h in a secondary
162 antibody solution of goat anti-mouse conjugated with Alexa 568 (1:500, Invitrogen, Thermo Fisher
163 Scientific), in PBS with 0.3% Triton and 2% normal horse serum. In all cases, one series of each
164 fifth section (sixth section in Case 71) was stained with the Nissl method (0.1% thionin in 0.1 M
165 acetate buffer, pH 3.7).

166

167 **Data analysis**

168 *Injection sites, distribution of retrogradely labeled neurons, and areal attribution of the labeling*

169 The criteria used for defining the injection site core and halo and identifying FB and CTBg labeling
170 have been described in earlier studies (Luppino et al. 2003; Rozzi et al., 2006). The injection sites

171 of Cases 71 and 75 were completely restricted to the putamen. In Case 61, the CTBg injection site
172 had some involvement ($<500\ \mu\text{m}$) of the white matter just above the putamen (Fig. 1). This white
173 matter involvement, given its minimal extent and location in close contact with the putamen and
174 considering that CTB is characterized by a limited uptake by axons of passage (Lanciego, 2015),
175 should not have affected the results from this case, which were fully comparable with those of the
176 other cases.

177 The distribution of retrograde labeling in the cortex was analyzed in sections every $300\ \mu\text{m}$
178 and plotted in sections every $1200\ \mu\text{m}$ (Cases 61, 71r, and 75) or $600\ \mu\text{m}$ (Cases 71l) together with
179 the outer and inner cortical borders, using a computer-based charting system. Data from individual
180 sections were also imported into the 3-dimensional (3D) reconstruction software (Demelio et al.
181 2001) providing volumetric reconstructions of the monkey brain, including connectional and
182 architectonic data.

183 The criteria and maps adopted for the areal attribution of the labeling were similar to those
184 adopted in previous studies (see Borra et al., 2017). Specifically, the attribution of the labeling to
185 the frontal motor, cingulate, and opercular frontal areas was made according to architectonic criteria
186 previously described (Matelli et al. 1985; 1991; Belmalih et al. 2009).

187 *Quantitative analysis and laminar distribution of the labeling*

188 In all cases, the number of labeled neurons plotted in the ipsilateral hemisphere was counted and the
189 cortical input to the injected putaminal zone was then expressed in terms of the percentage of
190 labeled neurons found in a given cortical subdivision, with respect to the overall cortical labeling
191 found for each tracer injection.

192 In all cases, the laminar distribution of the labeled cells was analyzed quantitatively in pairs or
193 triplets of close sections (spaced $300\text{-}600\ \mu\text{m}$), taken at different rostrocaudal levels through the
194 frontal motor and cingulate cortex and the frontal opercular cortex (Fig. 2). Given that in Cases 75
195 and 71r the labeling distribution was quite similar, the same levels (two sections/level) were
196 selected: the first level (A) was taken through F1, the second (B) through the caudal part of F3, the

197 third (C) through the middle part of F3 and the fourth (D) through the rostralmost part of F3. In
198 Case 61, the labeling involved more rostral cortical territories than in Cases 75 and 71r, thus the
199 caudalmost level analyzed was level B and it was possible to analyze a further rostral level (E)
200 through areas F6 and F7. In Case 711, the labeling was dense in relatively restricted cortical sectors,
201 thus the analysis was focused on these regions, at levels corresponding to B, C, and D, and was
202 carried out in two (level D) or three (levels B and C) sections spaced 600 μm .

203 Quantitative analysis was also carried out in parietal, insular, and prefrontal sectors selected
204 based on the distribution of the labeling in each case. For analyzing these regions, given that the
205 laminar distribution of the labeling was apparently very constant, cortical sectors of 2 mm from two
206 close sections (spaced 300-600 μm) were analyzed.

207 The selected sections were photographed at 100x magnification through a digital camera
208 incorporated into the microscope with an automatic acquisition system (NIS-Element; Nikon Co.,
209 Tokyo, Japan) and labeled neurons were plotted on the microphotographs. In the frontal sections of
210 Cases 61, 71r, and 75, the entire extent of the frontal motor and cingulate cortex and the opercular
211 frontal cortex was subdivided in 500 μm -wide cortical traverses perpendicular to the cortical
212 surface and running through the entire cortical thickness, from the pial surface to the grey-white
213 matter border. The width of the traverses was defined along a line running at the level of the layers
214 III-V border. In the frontal sections of Case 711 and in the sections through the parietal, insular, and
215 prefrontal cortex in all cases, where the labeling was in general less rich, cortical traverses 1 mm-
216 wide were defined in limited cortical sectors. Furthermore, microphotographs of immediately
217 adjacent Nissl-stained sections were overlaid and borders between different cortical layers were
218 then transferred on the plots. Two types of analyses were carried out on the distribution of the
219 labeled neurons. The first analysis aimed to obtain an estimate of the variations in overall richness
220 of the labeling within and across the various labeled cortical sectors. To this purpose, we have first
221 considered the total number of labeled cells observed in each traverse, in the entire cortical
222 thickness. Then, to compensate for differences in the number of labeled cells due to variations of

223 the cortical thickness between different areas or to oblique cutting of the cortical mantle, the total
224 number of labeled cells was divided by the cortical thickness, measured from the pial surface to the
225 grey-white matter border, expressed in millimeters. Thus, the richness of the labeling (“density”)
226 was expressed for each traverse in terms of number of labeled cells/mm cortical thickness. The
227 second analysis aimed to quantify the proportion of CSt labeled cells observed in the various layers.
228 To this aim, for each traverse the labeling was expressed in terms of percentage of labeled neurons
229 localized in layers II-III, V, and VI.

230 The distribution of labeled neurons was also analyzed qualitatively across consecutive
231 sections to exclude the possibility that the observed laminar distribution patterns of the labeling
232 were only apparent, because of an oblique cutting of the cortical mantle.

233

234 **RESULTS**235 **Location of the injection sites and general distribution of labeled CST neurons in the**
236 **ipsilateral hemisphere**

237 All injections used for this study involved the putaminal region overlying the crossing of the
238 anterior commissure (AC) at different dorso-ventral levels (Table 1 and Fig. 1). In Cases 75 and 71r
239 the injection sites were located in a dorsal and a mid-dorsal part of the putamen, respectively, at
240 about the antero-posterior (AP) level of the AC (Case 75), or slightly rostral (case 71r). According
241 to the putaminal motor somatotopy (e.g., Alexander and De Long, 1985; Nambu 2011) the injection
242 site in Case 75 could correspond mostly to the trunk-leg motor representation and in Case 71r to the
243 arm and trunk-leg motor representation. In Cases 71l and 61, the injection sites were located more
244 ventrally in the putamen, 2 mm caudal and 1 mm rostral to the center of the AC, respectively. In
245 Case 71l, the injection site could overlap with the hand and mouth motor representation. In Case 61,
246 it extended for about 4 mm in dorso-ventral direction and the ventral part could at least partially
247 overlap with the rostral “hand-related input channel” (Gerbella et al., 2016).

248 As expected, in all cases the majority of labeled cells was located in frontal motor areas (57-
249 75% of the labeled cells; Table 2) with additional, in several cases relatively robust, projections
250 from other cortical regions and their distribution in the ipsilateral hemisphere largely varied
251 depending on the location of the injection site (Figs. 2 and 3).

252 In Cases 75 and 71r the regional distribution of the labeling was quite similar: in both cases
253 about 62% of the labeled cells were located within frontal motor areas, about 19-22% in the
254 cingulate cortex and about 12-17% in the parietal cortex. In both cases the strongest input originated
255 from F1 (primary motor cortex), mostly from the dorsal and medial part, and a very rich labeling
256 involved the entire extent of F3 (supplementary motor area) and area 24c/d (cingulate motor areas)
257 mostly in the caudal part, corresponding to area 24d (Table 3). Relatively strong projections
258 originated also from F2 and, in Case 71r, in which the injection site extended more ventrally, also

259 from F5. In the parietal cortex, in both cases most of the labeling was in the dorsal part of areas SI
260 and PE and, in Case 71r, also in area PFG.

261 In Case 71l, the labeling was much weaker in the cingulate cortex and mostly confined to the
262 frontal motor (76%) and parietal (19%) cortex (Table 2). In the frontal cortex, the labeling was very
263 strong in the ventral premotor cortex, mostly in F5, also extending in the frontal operculum, and in
264 the mid-ventral part of F1 (Table 3), as expected from the location of the injection site. Relatively
265 robust labeling was observed in the rostral part of F3, likely involving the arm and face
266 representation (Luppino et al., 1991). In the parietal cortex, labeled cells were mostly distributed in
267 the ventral part of SI, and in SII, PF, PFG, and AIP.

268 In Case 61, the cortical labeling was more extensive than in the other three cases, likely
269 because of its more rostral location and relatively large dorsoventral extent. Specifically, the
270 labeling very densely involved the ventral premotor, the ventrolateral prefrontal cortex and the IPL
271 areas PFG, PG and AIP, which likely reflects involvement of the rostral “hand-related input
272 channel”. The labeling densely involved also F3 (mostly the mid-rostral part), F2, and 24c/d and,
273 less densely, areas F6, 24a/b and the insula (Tables 2 and 3).

274

275 **Laminar distribution of CSt labeled cells in the frontal motor, cingulate and frontal opercular** 276 **cortex**

277 As shown in detail below, in general the laminar distribution pattern of the labeled CSt cells in the
278 frontal motor and opercular cortex markedly differed across the various labeled zones and very
279 rarely showed the pattern commonly described in the primate brain, characterized by CSt cells
280 almost completely confined to layer V. For example, in the frontal motor cortex, in only 8% of the
281 1009 cortical bins (500 μ m wide) analyzed in 36 sections from all cases, labeled cells in layer V
282 were >66% and in 58% of the bins they were <50%. Indeed, labeled cells almost everywhere in
283 these regions tended to distribute over almost the entire cortical depth, involving, at a variable

284 extent, layers III, V, and VI. Noteworthy, there were also labeled CSt neurons in the underlying
285 white matter, which have been described in a previous study (Borra et al., 2020).

286 Figure 4 shows the results of the quantitative analysis carried out in sections through F1,
287 which was very richly labeled in Cases 75, 71r, and 71l. In sections sampled from Cases 75 and 71r,
288 taken caudally in F1 (Level A, in Figs. 2 and 3), in the granular cingulate area 23 the labeling by far
289 predominantly involved layer V, as in most of the sampled bins labeled cells in this layer were
290 >80% in Case 75 and >90% in Case 71r (Fig. 5A and B). In Case 75, at the transition of area 23
291 with F1, the laminar distribution pattern radically changed, as the proportion of labeled cells in
292 layers III and VI increased considerably (Fig 5C). For example, in section 108 there were about 12-
293 13 mm (bins 16-41) in which the proportion of layer V labeled cells was about 40% and that of
294 either layer III or layer VI was about 30%, whereas in section 109 the proportion of layer VI labeled
295 cells tended to be about 20%. Interestingly, this pattern remained unchanged despite clear changes
296 in labeling density, even when it abruptly halved in the range of very few bins (e.g., bins 28-31 in
297 section 108). In case 71r, the laminar distribution pattern in a sector of F1 similar to that sampled in
298 Case 75, was somewhat different: the proportion of labeled cells in layer V tended to be higher than
299 that in layers III and VI, though remaining for the whole extent of F1 in both the sampled sections
300 at about 50%. In case 71l, F1 was sampled in a triplet of close sections in a more lateral part (Level
301 B in Figs. 2 and 3), mostly in the bank of the central sulcus, where the labeling in this area was
302 richest. In all the three samples, the proportion of labeled cells in layer VI tended to be quite low,
303 but that in layer III was as high or, in several bins, even higher than in layer V, being above 50% in
304 8 mm out of 13 mm sampled (Fig 5E). A similar pattern was also observed in bins located in the
305 bank of the central sulcus in Case 75.

306 In all cases, layer V labeled cells in F1 were all relatively small and tended to be densely
307 packed mainly in the upper part of the layer, corresponding to sublayer Va. In Case 75, SMI-32
308 immunofluorescence, which reveals neurofilament proteins expressed in subpopulations of layers
309 III and V pyramids (Hof and Morrison, 1995), including the larger ones in layer Vb in the frontal

310 motor cortex (Geyer et al., 2000; Belmalih et al., 2009), showed that CTBg labeled neurons, though
311 invading layer Vb, were considerably smaller than larger SMI-32-immunopositive pyramids (cfr.
312 Fig. 5C and D). The analysis of these double-labeled sections also clearly showed that a high
313 proportion of CTBg labeled cells was located well below the large layer Vb pyramids, in layer VI.

314 Rostral to F1, the cingulate area 24c/d and the medial premotor cortex corresponding to F3
315 were sampled at different AP levels together with the adjacent sectors of F1 or F2 (Levels B, C, and
316 D; Figs. 6-8). Figure 7 shows the results of the analysis carried out in pairs of sections taken in all
317 cases at about the middle of F3, possibly corresponding to the arm representation of this area (Level
318 C). In area 24c/d, labeled cells were mainly located in layer V, although, especially in Case 61, in
319 several bins the proportion of cells located in layers III and VI was about 40%. In Cases 75 and 71r,
320 the laminar distribution pattern of labeled cells in F3 (Fig. 5F) was substantially similar to that
321 observed in F1. In Case 61, the percentage of layer V labeled cells was in most of the bins around
322 40%, in layer III tended to match that of layer V, whereas in layer VI it was lower and quite
323 variable. In Case 71l, relatively dense labeling was observed in a restricted zone in the mid-rostral
324 part of F3. Here, in two out of three sampled sections, labeled cells tended to be located mainly in
325 layer V (about 60%), whereas in one section the proportion of labeled cells in layer VI matched that
326 in layer V. In F2, the density of labeled cells tended to be lower than in F3 and their laminar
327 distribution tended to be similar to that observed in F3, though more variable across bins. Similar
328 laminar distribution patterns were observed in Cases 75, 71r and 61 in the caudal part of areas 24c/d
329 and F3 (Level B; Fig. 6).

330 At Level D (Figs. 2 and 3), through the rostralmost part of F3, at the border with F6, a
331 different laminar distribution pattern was observed in Cases 75 and 71r, characterized by a clear
332 increase in the percentage of labeled cells in layer V, compared to the more caudal levels (Fig. 8).
333 In Case 61, about 40-50% of the labeled cells was located in layer V and the remaining were almost
334 equally subdivided in layers III and VI.

335 An additional more rostral level (Level E) was sampled in Case 61 through areas 24c/d and
336 F6, where rich labeling was located (Fig. 9). The laminar distribution of the labeling was similar to
337 that observed more caudally in area 24c/d and rostral F3.

338 Accordingly, as observed for F1, there were differences in the laminar origin of CST
339 projections from medial and dorsal premotor areas, which were not correlated with the density of
340 the labeling, but likely with the target putaminal zone.

341 In three cases (61, 71r and 71l) there was rich labeling also in the ventral premotor cortex
342 (Fig. 10). In Case 61, the laminar distribution of the labeled cells in this region was examined
343 through F5 and the frontal operculum (levels D and E) and more caudally through F4 (Level C). In
344 Cases 71l and 71r, the labeling was rich in restricted zones of F5 and F4, which were sampled at
345 levels D and C, respectively. In Case 61, in the F5 sector buried within the postarcuate bank
346 (subdivision F5a) labeled cells were by far predominantly located in layer V. This pattern markedly
347 changed in the F5 sector extending on the convexity cortex (subdivision F5c), where the percentage
348 of labeled cells located in layer VI considerably increased, matching in several bins that of layer V
349 (around 40%; Fig. 5G). More ventrally, in the frontal operculum, at Level E, the contribution of
350 layer VI further increased, reaching in most of the bins percent values of at least 60%, whereas
351 more caudally (Level D) tended to be similar to that observed for F5c. In F5c and in the frontal
352 operculum, as well as in all the other frontal motor areas, labeled cells in layer VI, tended to be
353 more concentrated in the upper part of the layer and included pyramidal and non-pyramidal neurons
354 (Fig. 5H). Finally, in F4 (Level C) about 50% of the labeled cells was in layer V.

355 In Cases 71l and 71r, the laminar distribution pattern observed in F5a (both cases) and in F4
356 (Case 71r) was very similar to that described for Case 61. In contrast, the laminar distribution
357 pattern observed in F5c in Case 71l was markedly different from that observed in Case 61: the
358 percentage of labeled cells in layer V was by far predominant and that of layer VI was about 10%.
359 This observation was a further clear example that a given premotor area can project to different
360 parts of the motor putamen with a differential contribution of the various cortical layers.

361

362 **Laminar distribution of CSt labeled cells in the parietal, insular, and prefrontal cortex**

363 Differently from what was observed in the frontal motor and cingulate cortex and in the frontal
364 opercular cortex, in the parietal and insular cortex the laminar distribution of the CSt labeled cells
365 was substantially uniform and characterized by pyramidal cells predominantly confined to layer V,
366 with some of them in the position of layer IV. Specifically, in the parietal cortex, independently
367 from the labeled area and from the richness of the labeling, labeled cells in layer V (plus layer IV)
368 tended to be almost everywhere >80%, with the remaining mostly localized in layer VI (Fig. 5J). In
369 the insular cortex, labeled cells were by far predominantly located in layer V in Cases 75, 71r, and
370 71l in which the labeling was relatively poor. In Case 61, in which labeling in the insula was
371 considerably richer, most of the labeled cells was located in layer V and a variable, but robust
372 proportion was located in layer VI. This same case was the only one in which relatively rich
373 labeling was observed in the ventrolateral prefrontal cortex, more densely involving areas 46v and
374 12r. In this region, the majority of the labeled cells was located in layer V, but as observed in the
375 insular cortex, there was a relatively robust contribution (up to 40% of the labeled cells) of layer VI
376 (Fig. 5I).

377

378 **DISCUSSION**

379 The present study shows that CST projections from frontal motor areas and frontal operculum do not
380 originate almost exclusively from layer V, as commonly assumed in primate models of CST
381 interactions, as almost everywhere in these regions the contribution of layers III and VI to these
382 projections is comparable or even stronger than that of layer V. Furthermore, laminar distribution
383 patterns of the CST projections can largely vary within these regions independently from the
384 richness of the projections and from the projecting area/field, but likely according to the target
385 striatal zones.

386 Thus, cortical areas appear to project in different ways to different zones of the striatum, so
387 that different striatal zones are targets of characteristically weighted laminar projections from the
388 various input areas. These observations extend current models of CST interactions and provide an
389 even more complex picture of the possible mode of information processing in the basal ganglia for
390 motor and non-motor functions.

391

392 **Laminar origin of CST projections**

393 The laminar origin of CST projections has been described in several studies, showing differences
394 across species. In cats, CST neurons were observed mostly in layer III (Kitai et al 1976; Oka, 1980;
395 Royce, 1982), whereas in dogs mostly in layer V or III in prefrontal and motor cortex, respectively
396 (Tanaka, 1987). In rats, CST neurons have been observed mostly in layer V, and at a variable extent
397 across studies in layer III (e.g., Veening, 1980; McGeorge and Faull, 1989; Akitunde and Buxton,
398 1992; Wall, 2013). In macaques, after putaminal injections, CST neurons in the motor cortex were
399 described almost exclusively in layer Va (Jones et al, 1977), or primarily in layer Va, but also in
400 layers III and Vb (Mc Farland and Haber, 2000; Kaneda et al 2002). After caudate injections, the
401 labeling in prefrontal cortex was observed primarily in layer V, with a minor contribution from
402 layer III, correlated with labeling density (Arikuni and Kubota, 1986; Goldmann Rakic and
403 Selemon, 1986; Saint-Cyr et al 1990; Yeterian and Pandya 1994; Ferry et al., 2000). It is worth

404 noting that in all these studies the laminar distribution of CSt labeled cells has been evaluated only
405 qualitatively, which could be at the basis of an underestimation of the involvement of layers III and
406 VI. Furthermore, the lack of quantitative analysis in virtually all studies of CSt projections prevents
407 comparisons of the contribution of the various layers across different areas, tracer injections and
408 studies.

409 The commonly assumed notion that CSt neurons in the macaque brain are primarily located in
410 layer V (Gerfen and Bolam, 2010; Shepherd, 2013) has been challenged by Griggs et al. (2017).
411 This study showed that projections from specific temporal areas to the caudate head originated
412 mostly from layer V and occasionally from layer III, whereas projections from the same areas to the
413 caudate tail originated from layers III and VI. Accordingly, this study first showed that laminar
414 distribution patterns of CSt projections from a given cortical area can markedly differ according to
415 the target striatal zone and that, in macaques, layer VI can be a relevant source of CSt projections.

416 Present data, based on quantitative analysis of the laminar distribution of CSt neurons,
417 confirm and extend these observations showing that also in the frontal motor and in the frontal
418 opercular cortex CSt neurons are not located primarily in layer V and that layer VI can be a major
419 source of CSt projections (e.g., area F5c in Case 61). Labeled CSt neurons in layer VI in ventral
420 premotor cortex were noticed also by McFarland and Haber (2000). Finally, the present data show
421 that also after tracer injections in different parts of the putamen, different laminar distribution
422 patterns can be observed in a given cortical area. For example, after the injections in Case 61 and in
423 Case 711, the laminar distribution patterns of the labeled neurons in area F5 were markedly
424 different. Laminar distribution patterns can differ also across different fields of the same area, as
425 observed in F1 and F3. Noteworthy, these patterns did not change depending on the richness of the
426 labeling. Thus, similarly to the temporal cortex, in the motor cortex laminar distribution patterns of
427 CSt projections appear to vary according to the target striatal zone.

428 Present data, as well as those of Griggs et al (2017) raise the question of whether this new
429 model of laminar architecture of CSt projections applies also to other cortical regions. In parietal

430 and cingulate cortex, CSt labeled cells involved almost exclusively or predominantly layer V.
431 Although the putamen is a major target of CSt parietal projections (Yeterian and Pandya, 1993;
432 Cavada and Goldman-Rakic, 1991), we cannot rule out the possibility that projections to the
433 caudate originate also from other layers. In the insular cortex, we observed labeled CSt neurons in
434 layers V, or V-VI, and Chikama et al. (1997), after injections in the ventral striatum, observed
435 labeling in the agranular insula involving layer III. In the prefrontal cortex, Griggs et al (2017)
436 observed differences in CSt projections from layer III to the caudate tail and head and in the present
437 study we observed CSt neurons mainly in layers V and VI. Accordingly, it seems possible that also
438 in the prefrontal and insular cortex laminar distribution patterns of CSt projections vary according
439 to the target striatal zone.

440

441 **Functional considerations**

442 Previous data suggested that specific striatal zones are targets of converging input from
443 interconnected cortical areas, thus are integral part of specific large-scale functionally specialized
444 networks (Gerbella et al. 2016; Choi et al., 2017a, 2017b). Present data show that cortical areas may
445 project in different ways to different striatal zones, suggesting that they are targets of specific
446 combinations of signals originating from the various cortical layers of the areas of a given network.

447 These observations extend current models of CSt interactions, suggesting much more
448 complex modes of information processing in the basal ganglia for different motor and non-motor
449 functions, and opening new questions on the architecture of the CSt circuitry.

450 Rodent studies provided evidence for different populations of neurons located in different
451 cortical layers and differentially involved in the CSt circuitry: intrathelencephalic neurons, located
452 in layers III and Va, which also project to other cortical areas, and pyramidal-tract neurons located
453 in layer Vb, which also project to brainstem and spinal cord (Reiner et al., 2010). However, the
454 presence of pyramidal-tract neurons in macaques, suggested by Parent and Parent (2006), is not
455 supported by electrophysiological data (Bauswein et al., 1989). Furthermore, Jones et al. (1977)

456 showed that CSt neurons are smaller than corticospinal neurons and in the present study we have
457 not observed large layer Vb labeled pyramids.

458 Rodent studies have also provided evidence for inhibitory Somatostatin or Parvalbumin
459 positive GABAergic CSt neurons located in layers III, V, and VI (Jinno e Kosaka, 2004; Lee et al.,
460 2014; Rock et al., 2016), which may differentially modulate striatal output and motor activity
461 (Meltzer et al., 2017). Though long-range projecting GABAergic cortical neurons have been
462 described in macaques by Tomioka and Rockland (2007), no evidence has been provided so far for
463 inhibitory CSt neurons. Double-labelling experiments will be necessary in order to verify whether
464 also in the macaque there are inhibitory CSt neurons as observed in rodents.

465 Current models of cortical circuitry suggest that the various cortical layers display distinct
466 responses and dynamics (see, Douglas and Martin 2004). Specifically, in the premotor cortex
467 activity generated by thalamic or cortical input first involves the middle layers and then superficial
468 and deep layers (Godlove et al., 2014) and in superficial layers neural activity is predominantly
469 related to choices, whereas in deeper layers to the motor output (Chandrasekaran et al., 2017).
470 Finally, in frontal areas deep layers appear to modulate the activity of the superficial layers related
471 to maintaining contents in working memory (Bastos et al., 2018).

472 Thus, different putaminal zones would collect signals originating from similar sets of hand-
473 related cortical areas, for example the “lateral grasping network”, but differing in term of coding
474 and timing even when originating from the same area. Furthermore, layers III, V and VI broadcast
475 signals in different directions (e.g., feed-forward, or feed-back) to other cortical areas of the
476 network. Accordingly, each striatal zone would be involved in a very specific way in the flow of
477 information within the cortico-subcortical network.

478 In this context, noteworthy is the observation that layer VI can be a robust source of CSt
479 projections. Layer VI hosts pyramidal neurons projecting to the thalamus (CT) or to other cortical
480 areas (CC; see Thompson, 2010). It is thus an open question whether pyramidal layer VI CSt
481 neurons observed in the present study represent a new class of layer VI pyramids, or they belong to

482 the CT and/or the CC types. After tracer injections in the thalamus and in the caudate, Yeterian and
483 Pandya (1994) did not find double-labeled neurons in the prefrontal cortex, where CSt labeled cells
484 were observed almost exclusively in layer V. Thus, this study does not rule out the possibility that
485 there are indeed layer VI CSt neurons which also project to the thalamus. Accordingly, it is possible
486 that striatal zones receive from layer VI neurons signals, which are sent also as feed-back signals
487 either to cortical areas of the network and/or to thalamic nuclei, possibly to the basal ganglia
488 recipient ones. Further studies are necessary to characterize connectionally and neurochemically
489 layer VI CSt neurons and to define the possible role of this projection in the basal ganglia circuitry.
490

491 **REFERENCES**

492 Akintunde A, Buxton DF (1992) Origins and collateralization of corticospinal, corticopontine,
493 corticorubral and corticostriatal tracts: a multiple retrograde fluorescent tracing study. *Brain Res.*
494 586:208–218.

495 Alexander GE, DeLong MR (1985) Microstimulation of the primate neostriatum. II.
496 Somatotopic organization of striatal microexcitable zones and their relation to neuronal response
497 properties. *J Neurophysiol.* 53:1417–1430.

498 Alexander GE, DeLong MR, Strick PL (1986) Parallel organization of functionally segregated
499 circuits linking basal ganglia and cortex. *Annu Rev Neurosci.* 9:357–381.

500 Arikuni T, Kubota K. (1986) The organization of prefrontocaudate projections and their laminar
501 origin in the macaque monkey: a retrograde study using HRP-gel. *J Comp Neurol.* 244:492–510.

502 Bastos AM, Loonis R, Kornblith S, Lundqvist M, Miller EK (2018) Laminar recordings in
503 frontal cortex suggest distinct layers for maintenance and control of working memory. *Proc Natl*
504 *Acad Sci U S A.* 115:1117–1122.

505 Bauswein E, Fromm C, Preuss A (1989) Corticostriatal cells in comparison with pyramidal tract
506 neurons: contrasting properties in the behaving monkey. *Brain Res.* 493:198–203.

507 Belmalih A, Borra E, Contini M, Gerbella M, Rozzi S, Luppino G (2009) Multimodal
508 architectonic subdivision of the rostral part (area F5) of the macaque ventral premotor cortex. *J*
509 *Comp Neurol* 512:183–217.

510 Borra E, Gerbella M, Rozzi S, Luppino G (2017) The macaque lateral grasping network: A
511 neural substrate for generating purposeful hand actions. *Neurosci Biobehav Rev.* 75:65–90.

512 Borra E, Luppino G, Gerbella M, Rozzi S, Rockland KS (2020) Projections to the putamen from
513 neurons located in the white matter and the claustrum in the macaque. *J Comp Neurol* 528, 453–467

- 514 Cavada C, Goldman-Rakic PS (1991) Topographic segregation of corticostriatal projections
515 from posterior parietal subdivisions in the macaque monkey. *Neuroscience*. 42:683–696.
- 516 Chandrasekaran C, Peixoto D, Newsome WT, Shenoy KV (2017) Laminar differences in
517 decision-related neural activity in dorsal premotor cortex. *Nat Commun*. 8:614. Published 2017 Sep
518 20. doi:10.1038/s41467-017-00715-0
- 519 Chikama M, McFarland NR, Amaral DG, Haber SN (1997) Insular Cortical Projections to
520 Functional Regions of the Striatum Correlate with Cortical Cytoarchitectonic Organization in the
521 Primate *J Neurosci*. 17: 9686–9705.
- 522 Choi EY, Ding SL, Haber SN (2017a) Combinatorial inputs to the ventral striatum from the
523 temporal cortex, frontal cortex, and amygdala: implications for segmenting the striatum. *eNeuro*.
524 4:ENEURO.0392-17.2017.
- 525 Choi EY, Tanimura Y, Vage PR, Yates EH, Haber SN (2017b) Convergence of prefrontal and
526 parietal anatomical projections in a connectional hub in the striatum. *Neuroimage*. 146:821–832.
- 527 Demelio S, Bettio F, Gobbetti E, Luppino G. (2001) Three-dimensional reconstruction and
528 visualization of the cerebral cortex in primates. In: *Data visualization 2001* (Ebert D, Favre J,
529 Peikert R, eds) pp 147–156. New York, NY, USA: Springer Verlag.
- 530 Douglas RJ, Martin KA (2004) Neuronal circuits of the neocortex. *Annu Rev Neurosci*. 27:419–
531 451.
- 532 Ferry AT, Ongür D, An X, Price JL (2000) Prefrontal cortical projections to the striatum in
533 macaque monkeys: evidence for an organization related to prefrontal networks. *J Comp Neurol*.
534 425:447–470.
- 535 Gerbella M, Borra E, Mangiaracina C, Rozzi S, Luppino G (2016) Corticostriate Projections
536 from Areas of the "Lateral Grasping Network": Evidence for Multiple Hand-Related Input
537 Channels. *Cereb. Cortex* 221:59–78.

538 Gerfen CR, Bolam P (2010) The neuroanatomical organization of the basal ganglia. In:
539 Handbook of basal ganglia structure and function (Steiner H, Tseng KY, eds.), pp 3–32. London:
540 Academic Press.

541 Geyer S, Matelli M, Luppino G, Zilles K (2000) Functional neuroanatomy of the primate
542 isocortical motor system. *Anat Embryol* 202:443–474.

543 Godlove DC, Maier A, Woodman GF, Schall JD (2014) Microcircuitry of agranular frontal
544 cortex: testing the generality of the canonical cortical microcircuit. *J Neurosci.* 34:5355–5369.

545 Goldman-Rakic PS, Selemon LD (1986) Topography of Corticostriatal Projections in Nonhuman
546 Primates and Implications for Functional Parcellation of the Neostriatum. In *Sensory-Motor Areas*
547 *and Aspects of Cortical Connectivity* (Jones EG et al, eds), pp447–466. Plenum Press, New York.

548 Griggs WS, Kim HF, Ghazizadeh A, Costello MG, Wall KM, Hikosaka O (2017) Flexible and
549 Stable Value Coding Areas in Caudate Head and Tail Receive Anatomically Distinct Cortical and
550 Subcortical Inputs. *Front Neuroanat.* 11:106.

551 Hof PR, Morrison JH (1995) Neurofilament protein defines regional patterns of cortical
552 organization in the macaque monkey visual system: a quantitative immunohistochemical analysis. *J*
553 *Comp Neurol* 352:161–186.

554 Jinno S, Kosaka T (2004) Parvalbumin is expressed in glutamatergic and GABAergic
555 corticostriatal pathway in mice. *J Comp Neurol.* 477:188–201.

556 Jones EG, Coulter JD, Burton H, Porter R (1977) Cells of origin and terminal distribution of
557 corticostriatal fibers arising in the sensory-motor cortex of monkeys. *J Comp Neurol.* 173:53–80.

558 Kaneda K, Nambu A, Tokuno H, Takada M (2002) Differential processing patterns of motor
559 information via striatopallidal and striatonigral projections. *J Neurophysiol.* 88:1420–1432.

560 Kitai ST, Kocsis JD, Wood J (1976) Origin and characteristics of the cortico-caudate afferents:
561 an anatomical and electrophysiological study. *Brain Res.* 118:137–141.

562 Lanciego JL (2015) Retrograde Tract-Tracing “Plus”: Adding Extra Value to Retrogradely
563 Traced Neurons. In: *Neural Tracing Methods: Tracing Neurons and Their Connections* (Arenkiel
564 BL, ed), pp67-84. New York: Humana Press.

565 Lee AT, Vogt c D, Rubenstein JL, Sohal VS (2014) A class of GABAergic neurons in the
566 prefrontal cortex sends long-range projections to the nucleus accumbens and elicits acute avoidance
567 behavior. *J Neurosci.* 34:11519–11525.

568 Luppino G, Matelli M, Camarda RM, Gallese V, Rizzolatti G. (1991) Multiple representations of
569 body movements in mesial area 6 and the adjacent cingulate cortex: an intracortical
570 microstimulation study in the macaque monkey. *J Comp Neurol.* 311:463–482.

571 Luppino G, Rozzi S, Calzavara R, Matelli M (2003) Prefrontal and agranular cingulate
572 projections to the dorsal premotor areas F2 and F7 in the macaque monkey. *Eur J Neurosci* 17:559–
573 578.

574 Matelli M, Luppino G, Rizzolatti G (1985) Patterns of cytochrome oxidase activity in the frontal
575 agranular cortex of macaque monkey. *Behav Brain Res* 18:125–136.

576 Matelli M, Luppino G, Rizzolatti G (1991) Architecture of superior and mesial area 6 and the
577 adjacent cingulate cortex in the macaque monkey. *J Comp Neurol* 311:445–462.

578 McFarland NR, Haber SN (2000) Convergent inputs from thalamic motor nuclei and frontal
579 cortical areas to the dorsal striatum in the primate. *J Neurosci.* 20:3798–813.

580 McGeorge AJ, Faull RL (1989) The organization of the projection from the cerebral cortex to the
581 striatum in the rat. *Neuroscience.* 29:503–37.

- 582 Melzer S, Gil M, Koser DE, Michael M, Huang KW, Monyer H. (2017) Distinct corticostriatal
583 GABAergic neurons modulate striatal output neurons and motor activity. *Cell Rep.* 19:1045–1055.
- 584 Middleton FA, Strick PL (2000) Basal ganglia and cerebellar loops: motor and cognitive circuits.
585 *Brain Res Brain Res Rev.* 31:236–250.
- 586 Nambu A (2011) Somatotopic organization of the primate basal ganglia. *Front Neuroanat.* 5:26.
- 587 Oka H (1980) Organization of the cortico-caudate projections. A horseradish peroxidase study in
588 the cat. *Exp Brain Res.* 40:203–208.
- 589 Parent M, Parent A (2006) Single-axon tracing study of corticostriatal projections arising from
590 primary motor cortex in primates. *J Comp Neurol.* 496:202–213.
- 591 Pettine WW, Steinmetz NA, Moore T (2019) Laminar segregation of sensory coding and
592 behavioral readout in macaque V4. *Proc Natl Acad Sci U S A.* 116:14749–14754.
- 593 Reiner A, Hart NM, Lei W, Deng Y (2010) Corticostriatal projection neurons - dichotomous
594 types and dichotomous functions. *Front Neuroanat.* 4:142.
- 595 Reveley C, Gruslys A, Ye FQ, Samaha J, Glen D, Russ B, Saad Z, Seth A, Leopold DA, Saleem
596 KS (2017) Three-dimensional digital template atlas of the macaque brain. *Cereb Cortex* 27: 4463-
597 4477.
- 598 Rock C, Zurita H, Wilson C, Apicella AJ (2016) An inhibitory corticostriatal pathway. *Elife.* 9:5.
- 599 Royce GJ (1982) Laminar origin of cortical neurons which project upon the caudate nucleus: a
600 horseradish peroxidase investigation in the cat. *J Comp Neurol.* 205:8–29.
- 601 Rozzi S, Calzavara R, Belmalih A, Borra E, Gregoriou GG, Matelli M, Luppino G (2006)
602 Cortical connections of the inferior parietal cortical convexity of the macaque monkey. *Cereb*
603 *Cortex* 16:1389–1417.

604 Saint-Cyr JA, Ungerleider LG, Desimone R (1990) Organization of visual cortical inputs to the
605 striatum and subsequent outputs to the pallido-nigral complex in the monkey. *J Comp Neurol.*
606 298:129–156.

607 Shepherd GM (2013) Corticostriatal connectivity and its role in disease. *Nat Rev Neurosci*
608 14:278-291

609 Strick PL, Dum RP, Picard N (1995) Macro-organization of the circuits connecting the basal
610 ganglia with the cortical motor areas. In: *Models of information processing in the basal ganglia*
611 (Houk G, ed), pp117–130. Boston: MIT Press.

612 Takada M, Tokuno H, Nambu A, Inase M (1998) Corticostriatal projections from the somatic
613 motor areas of the frontal cortex in the macaque monkey: segregation versus overlap of input zones
614 from the primary motor cortex, the supplementary motor area, and the premotor cortex. *Exp Brain*
615 *Res.* 120:114–128.

616 Tanaka D Jr (1987) Differential laminar distribution of corticostriatal neurons in the prefrontal
617 and pericruciate gyri of the dog. *J Neurosci.* 7:4095–4106.

618 Thomson AM (2010) Neocortical layer 6, a review. *Front Neuroanat.* 4:13.

619 Tomioka R, Rockland KS (2007) Long-distance corticocortical GABAergic neurons in the adult
620 monkey white and gray matter. *J Comp Neurol.* 505:526–538.

621 Veening JG, Cornelissen FM, Lieven PA (1980) The topical organization of the afferents to the
622 caudatoputamen of the rat. A horseradish peroxidase study. *Neuroscience.* 5:1253–1268.

623 Wall NR, De La Parra M, Callaway EM, Kreitzer AC (2013) Differential innervation of direct-
624 and indirect-pathway striatal projection neurons. *Neuron.* 79:347–360.

625 Yeterian EH, Pandya DN (1993) Striatal connections of the parietal association cortices in rhesus
626 monkeys. *J Comp Neurol.* 332:175–997.

627 Yeterian EH, Pandya DN (1994) Laminar origin of striatal and thalamic projections of the
628 prefrontal cortex in rhesus monkeys. *Exp Brain Res.* 99:383–398.

629

630 **Table 1.** Animals used, location of injection sites in the putamen, and type and amount of injected
 631 tracers

Case	Species	Sex	Age	Weight	Hemisphere	AP*	Tracer	Amount
61	<i>M.Mulatta</i>	F	6	4.5	R	+1	CTBg 1%	2 µl
71	<i>M.Mulatta</i>	F	6.5	3.3	L	-2	FB 3%	0.3 µl
					R	+2	CTBg 1%	1 µl
75	<i>M.Mulatta</i>	M	6	3.5	R	0	CTBg 1%	1 µl

632 *AP level according to the digital atlas of Reveley et al., (2017) in which AP = 0 is at the level of
 633 the anterior commissure

634

635 **Table 2.** Regional distribution (%) and total number (n) of labeled neurons observed following
 636 tracer injections in the motor putamen

Case	Prefrontal	Cingulate	Frontal motor	Parietal	Insula	Temporal	n. cells
75	0,7	19,4	61,7	16,7	1,6	-	59653
71r	1,6	21,9	61,6	11,9	3	-	60757
71l	0,5	3,4	75,5	18,6	1,2	0,8	36628
61	8,4	18,3	57	7,5	6,1	2,7	105724

637

638 **Table 3.** Distribution (%) in the frontal and cingulate motor cortex and in the frontal operculum
 639 (FrOp) of labeled neurons observed following tracer injections in the motor putamen

Case	24c/d	F6	F7	F3	F2	FrOp	F5	F4	F1
75	14,4	0,8	0,3	12,7	7,1	2,2	2,5	2,0	34,1
71r	14,4	0,8	0,5	13,2	6,5	2,4	7,9	3,3	26,9
71l	2,5	0,1	-	6,9	0,7	7,6	33,4	8,2	18,6
61	12,3	3,7	1,2	10,6	9,3	16,5	10	3,0	2,7

640

641

642 **FIGURE LEGENDS**

643 **Figure 1.** Location of the injection sites. **Upper part:** drawings of coronal sections showing the
644 location of the injection sites in the putamen depicted as a black zone corresponding to the core,
645 surrounded by a grey zone corresponding to the halo. All sections are shown as from a right
646 hemisphere. The anteroposterior (AP) level of the sections is indicated in relation to the digital atlas
647 of Reveley et al. (2017) in which AP = 0 is at the level of the anterior commissure (AC). **Lower**
648 **part:** fluorescence photomicrographs of the injection sites in the putamen; scale bar in Case 75
649 applies to all. Dashed lines in the injection site of Case 61 indicate the deposit of the tracer in
650 adjacent sections. C, central sulcus; Cd, caudate nucleus; Cg, cingulate sulcus; GP, globus pallidus;
651 ic, internal capsule; L, lateral fissure; OT, optic tract; Pt, putamen; RTh, reticularis thalami; S, spur
652 of the arcuate sulcus; ST, superior temporal sulcus.

653 **Figure 2.** Distribution of the cortical labeling observed after injections in the putamen. The
654 distribution of the retrograde labeling is shown in dorsolateral and medial views of the 3D
655 reconstructions of the injected hemispheres in which each dot corresponds to one labeled neuron. In
656 each reconstruction, solid lines indicate the levels (A-E) of the sections selected for the quantitative
657 analysis. For the sake of comparison, also Case 711 is shown as right. FrOp, frontal operculum; IA,
658 inferior arcuate sulcus; IP, intraparietal sulcus; LO, lateral orbital sulcus; Lu, lunate sulcus; P,
659 principal sulcus; ParOp, parietal operculum; SA, superior arcuate sulcus. Other abbreviations as in
660 Figure 1.

661 **Figure 3.** Distribution of the cortical labeling in one representative section from each level selected
662 for the quantitative analysis. Section drawings are in a caudal to rostral order (A-E) and were taken
663 at the levels shown in Figure 2. Section number is indicated in brackets. Arrowheads indicate
664 borders of frontal motor areas. Subcortical labeling is not shown. A, amygdala; FEF, frontal eye
665 field; I, insula; ITG, inferior temporal gyrus; LG, lateral geniculate nucleus; Ri, retro-insular cortex;
666 STG, superior temporal gyrus; Th, thalamus. Other abbreviations as in Figures 1 and 2.

667 **Figure 4.** Percent laminar distribution and density of the retrograde labeling in F1. Graphs show
668 data from Cases 75, 71r (level A, 2 sections each) and 711 (level B, 3 sections). For each case, on
669 the left, one section drawing shows the analyzed cortical sector and layer V shaded in light blue.
670 Graphs from Cases 75 and 71r are aligned at the level of the fundus of the cingulate sulcus (a),
671 indicated by a vertical dashed line. The other vertical dashed lines indicate the level of the medial
672 edge of the hemisphere (b) and the shoulder of the central sulcus (c). Graphs from Case 75 and 71r
673 show data from 500 μm -wide bins from the region in which the labeled cell density was constantly
674 higher than 10 labeled cells/bin/mm. In graphs from Case 711, the bins are 1 mm-wide and located
675 in the lateral part of F1, in the bank of the central sulcus. Arrowheads indicate the location of areal
676 borders.

677 **Figure 5.** Examples of laminar distribution of the labeling. A, B (section 110), C, D (section 106)
678 and F (section 93) are from Case 75. B and D show the SMI-32 immunofluorescence in A and C,
679 respectively. E (section 98) is from Case 711. G (section 76, enlarged in H) and I are from Case 61.
680 J is from Case 71r.

681 **Figure 6.** Percent laminar distribution and density of the retrograde labeling in the cingulate and
682 frontal motor cortex at level B in Cases 75, 71r and 61. Conventions as in Figure 4.

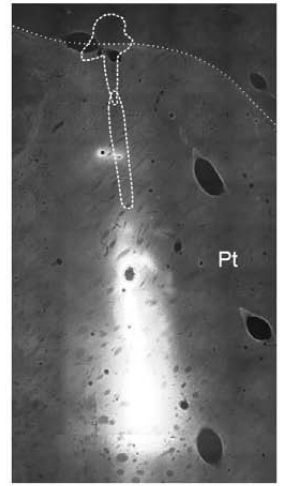
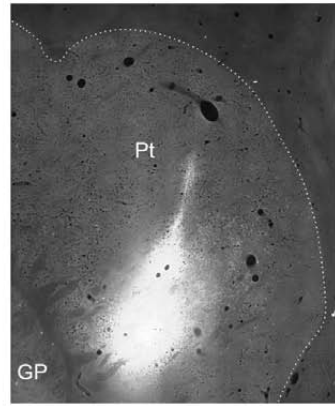
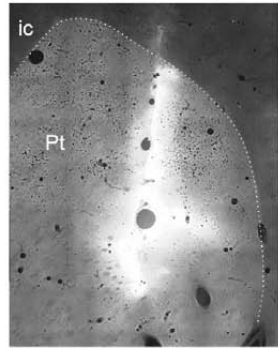
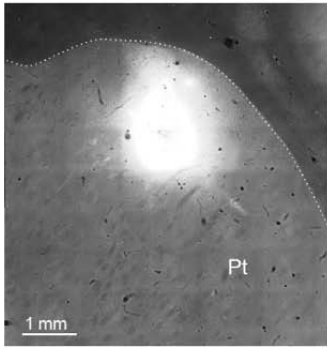
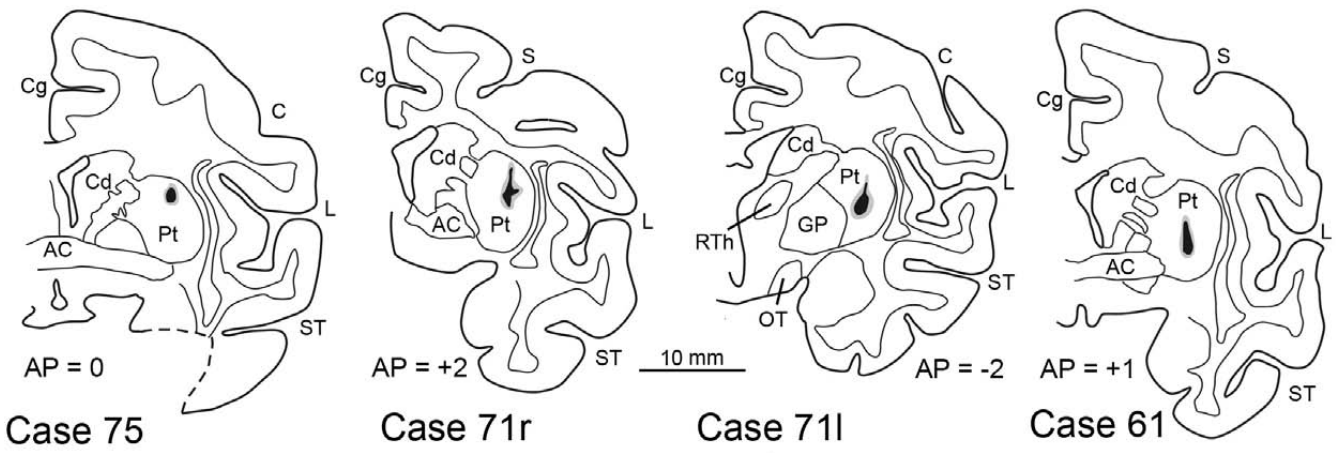
683 **Figure 7.** Percent laminar distribution and density of the retrograde labeling in the cingulate and
684 frontal motor cortex at level C, in all cases. Conventions as in Figure 4.

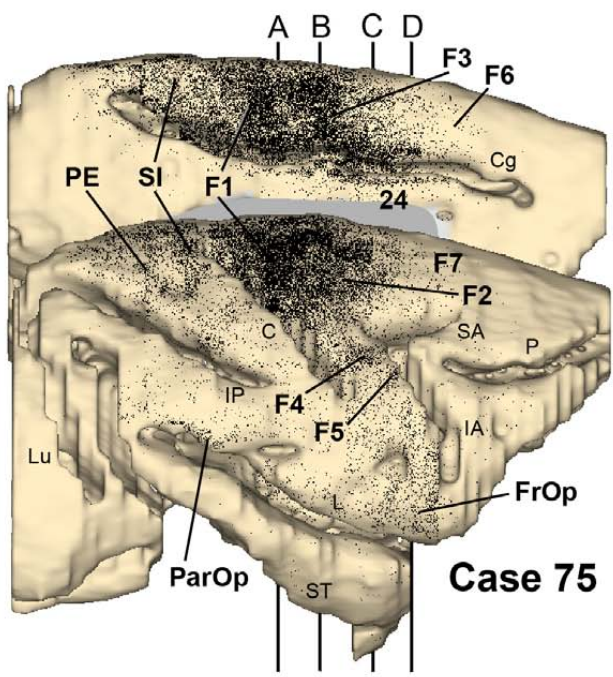
685 **Figure 8.** Percent laminar distribution and density of the retrograde labeling in the cingulate and
686 frontal motor cortex at level D, in Cases 75, 71r and 61. Conventions as in Figure 4.

687 **Figure 9.** Percent laminar distribution and density of the retrograde labeling in the cingulate and
688 frontal motor cortex at level E in Case 61. Conventions as in Figure 4.

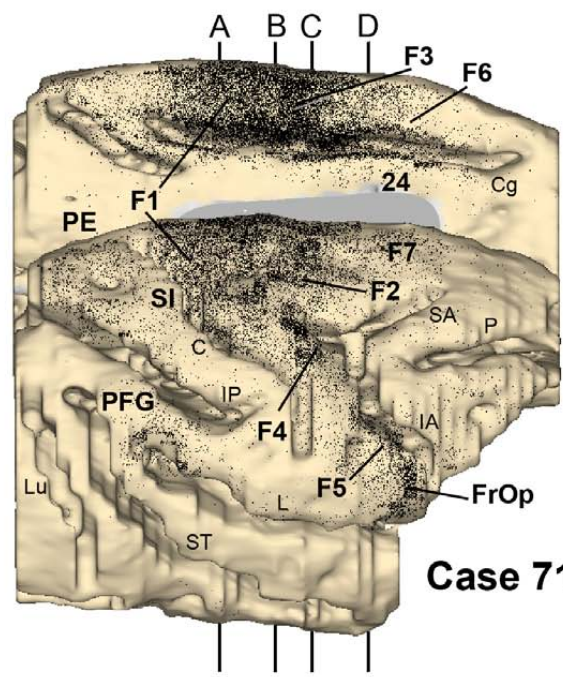
689 **Figure 10.** Percent laminar distribution and density of the retrograde labeling in the ventral
690 premotor and opercular frontal cortex. Graphs from Case 61 show data from a cortical region of

691 sections at levels E and D running from the fundus of the arcuate sulcus (left) through F5a, F5c, and
692 the frontal operculum and at level C through F4 on the convexity cortex. Graphs from Case 711
693 show data from cortical sectors 3 mm wide of sections taken at level D within the arcuate bank
694 (F5a) or on the convexity cortex (F5c). Graphs from Case 71r show data from cortical sectors taken
695 at level D (in F5a) and level C (in F4) in which the density of labeled cells was above 10
696 cells/bin/mm. Conventions as in Figure 4.

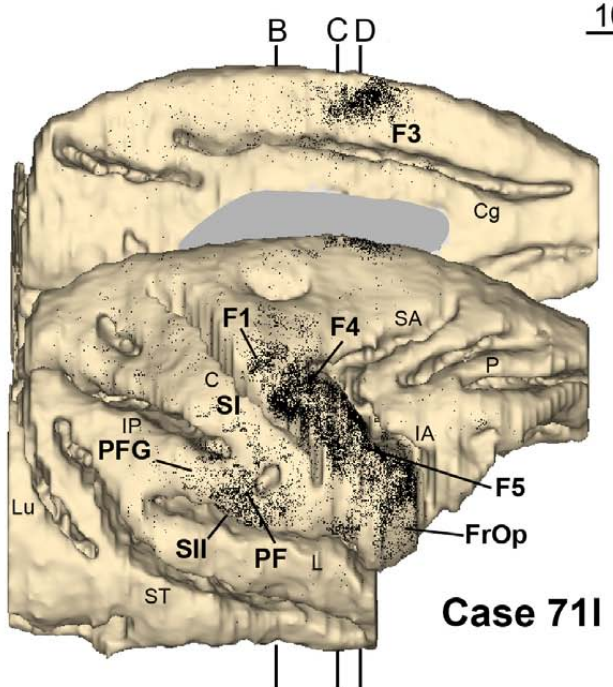




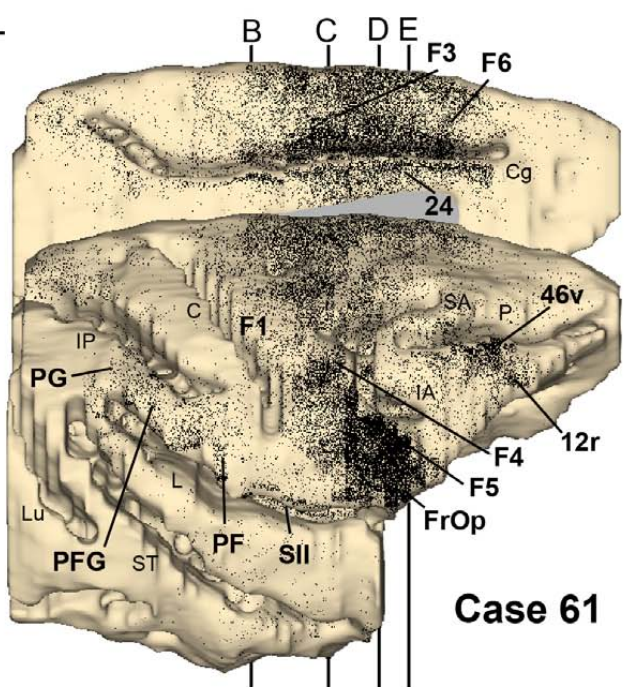
Case 75



Case 71r

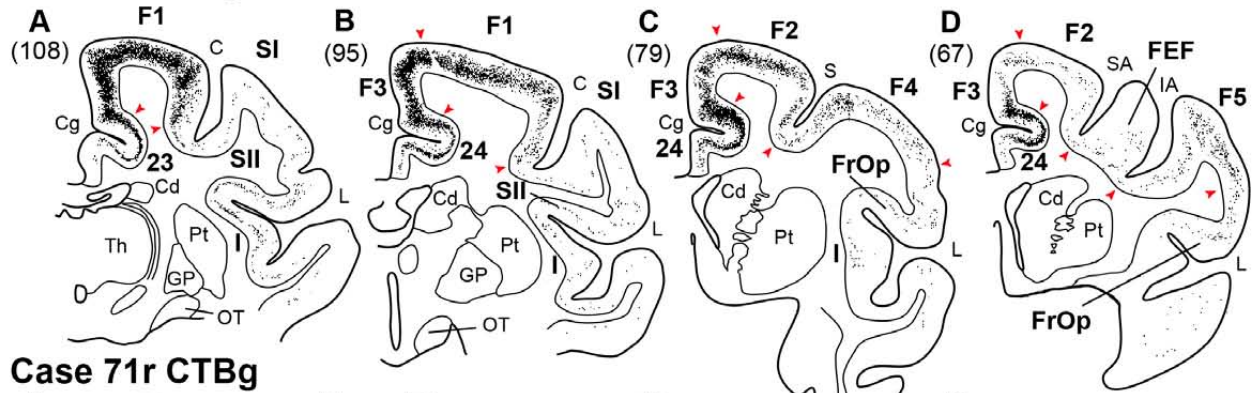


Case 71l

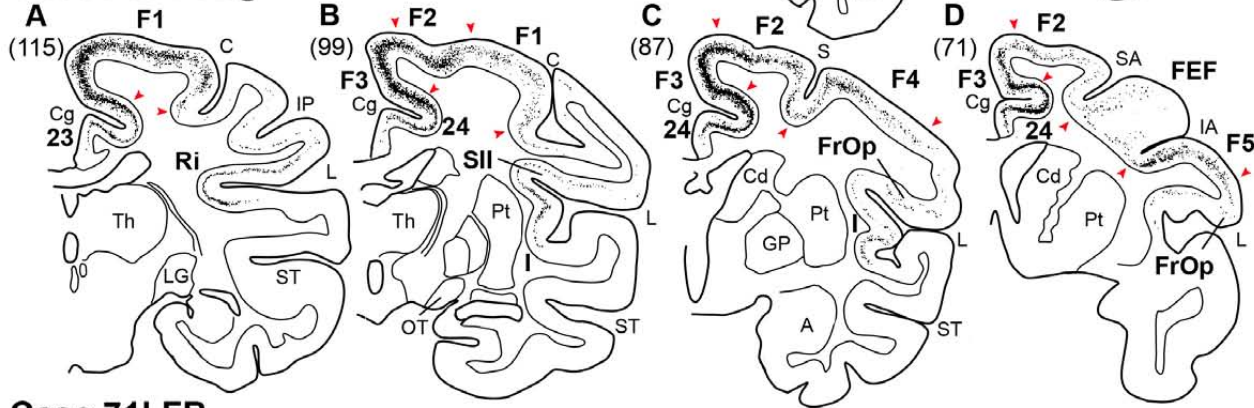


Case 61

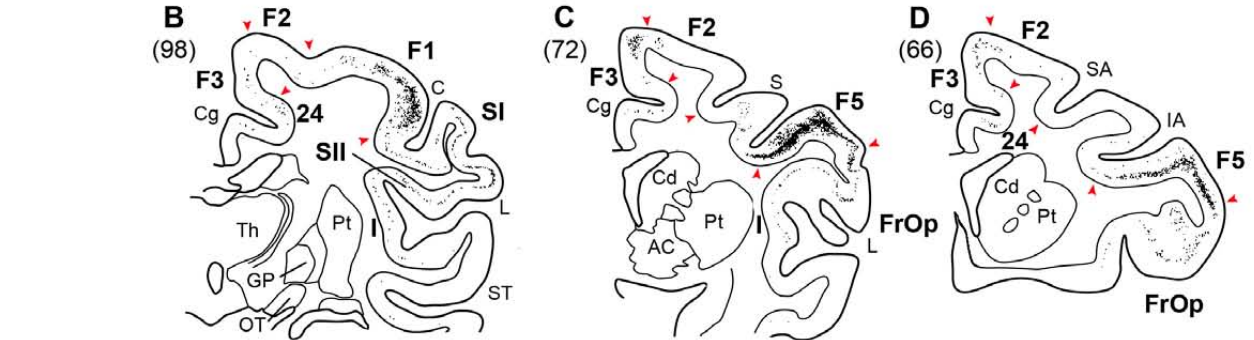
Case 75 CTBg



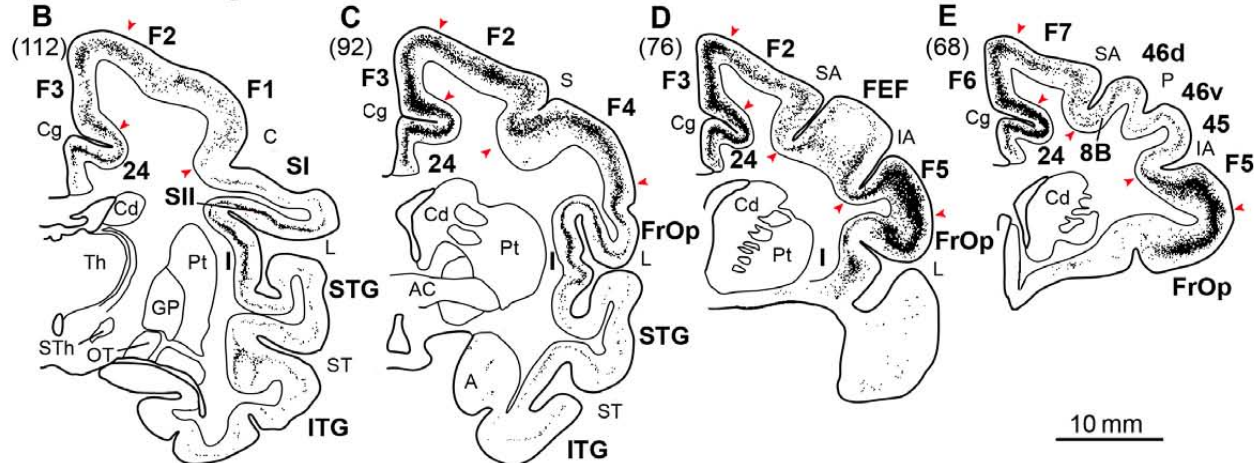
Case 71r CTBg

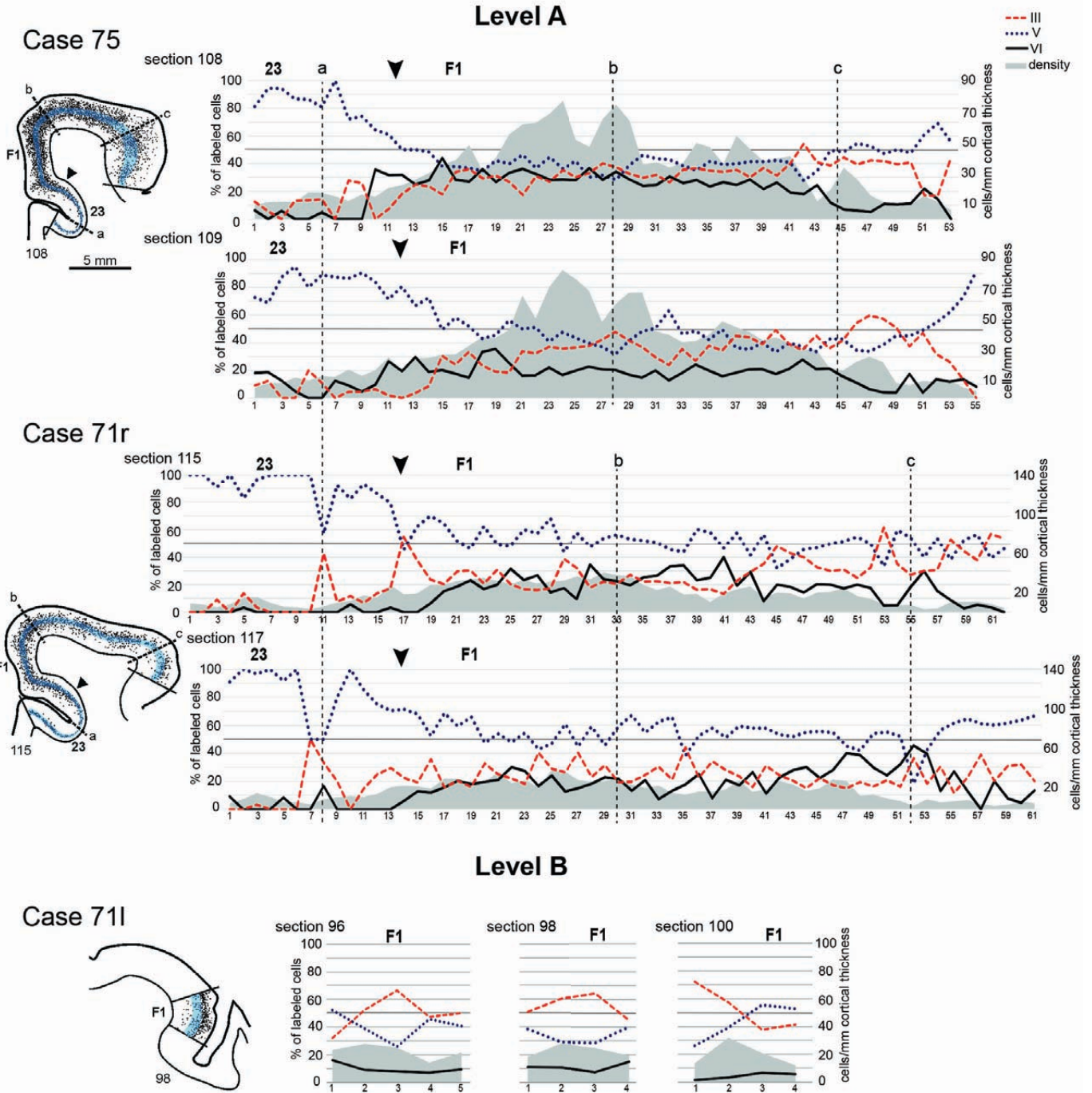


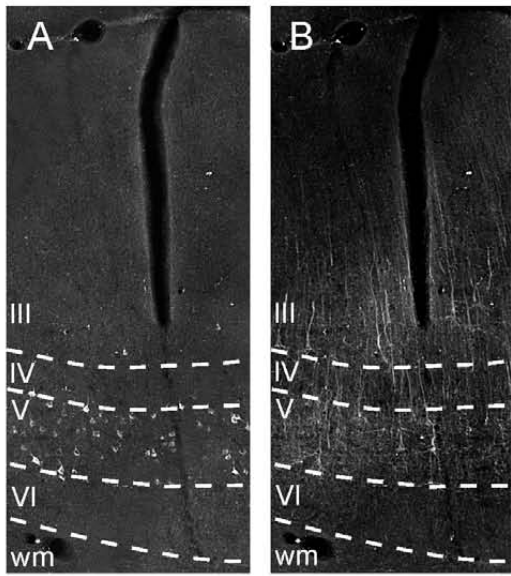
Case 71l FB



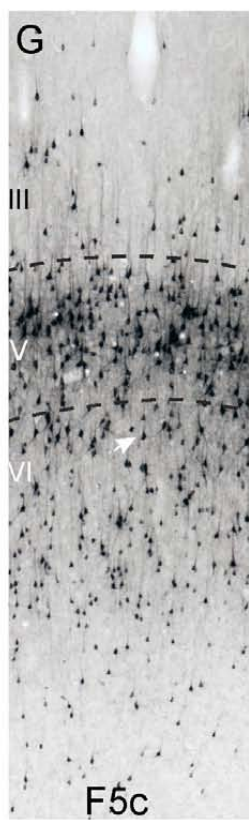
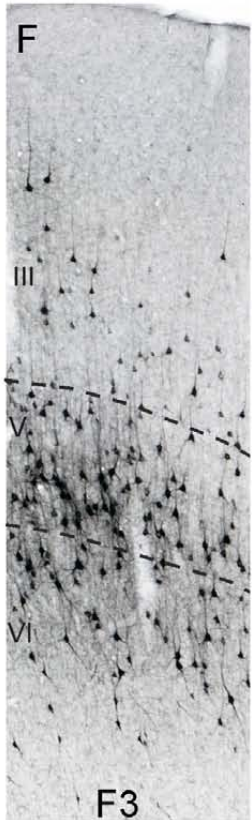
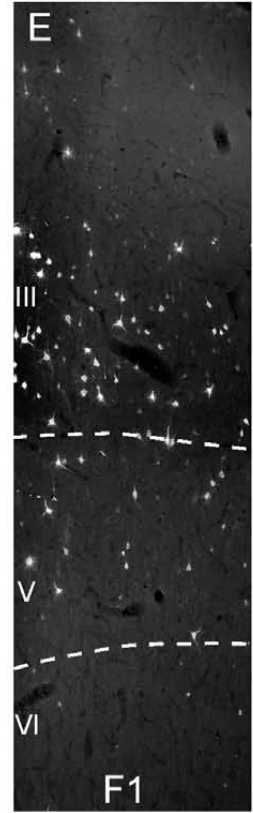
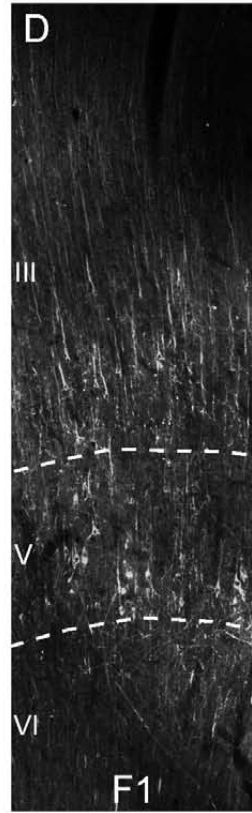
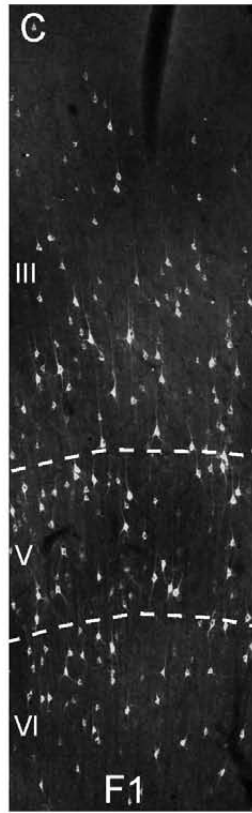
Case 61 CTBg



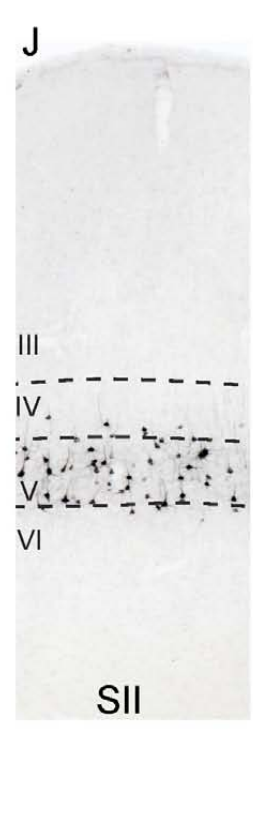
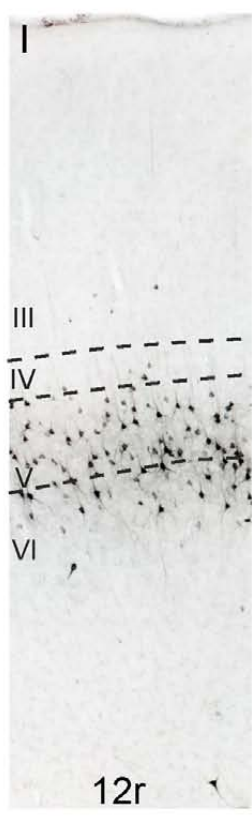




23 0.5 mm 23

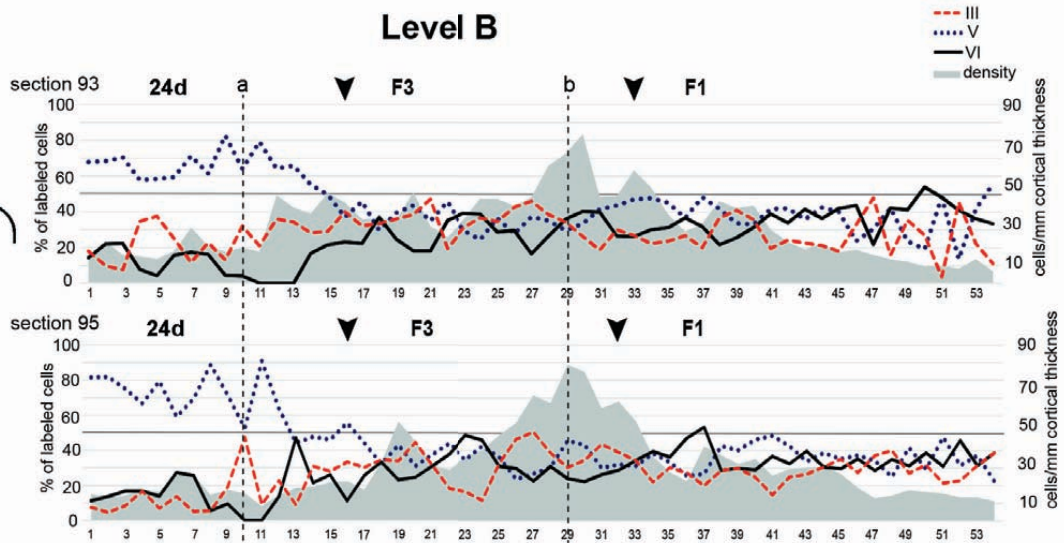
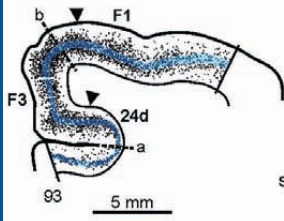


0.25 mm

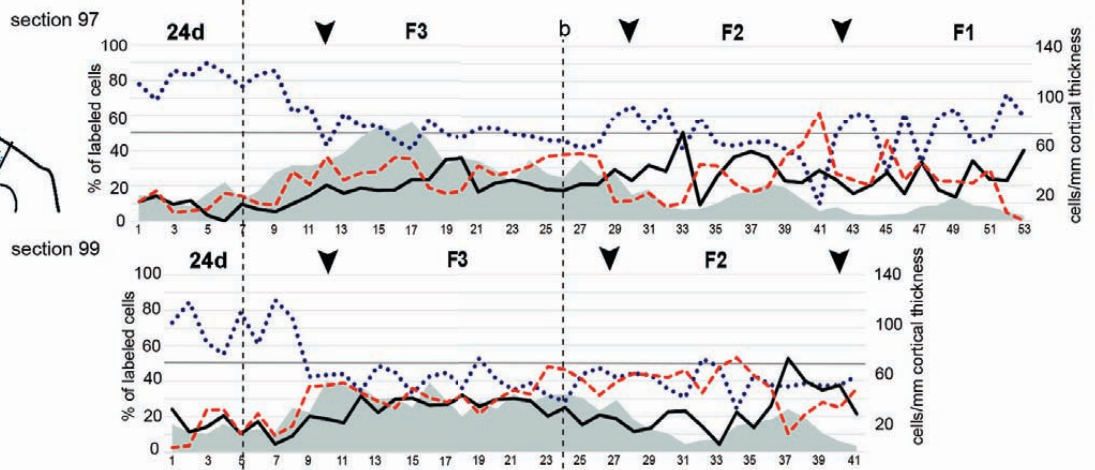
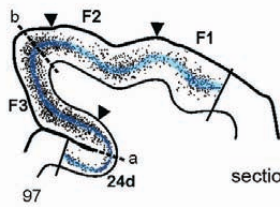


Case 75

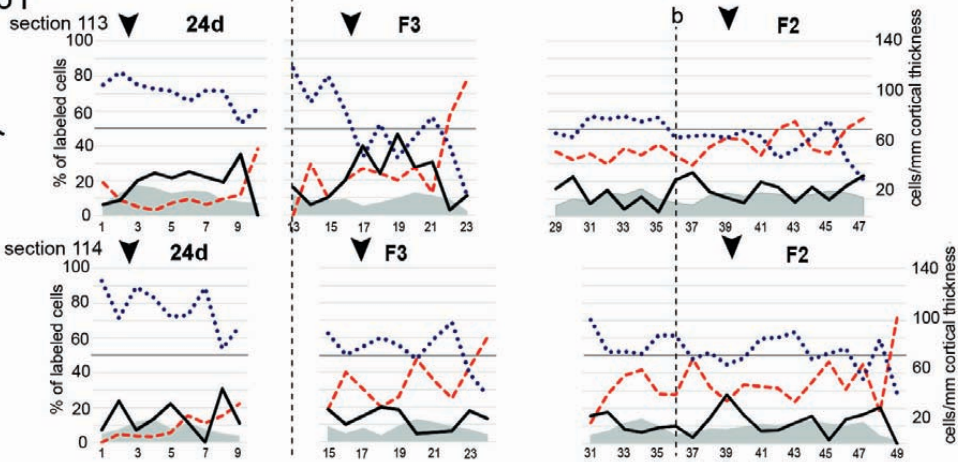
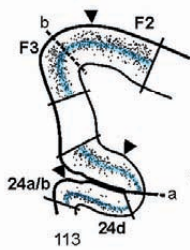
Level B

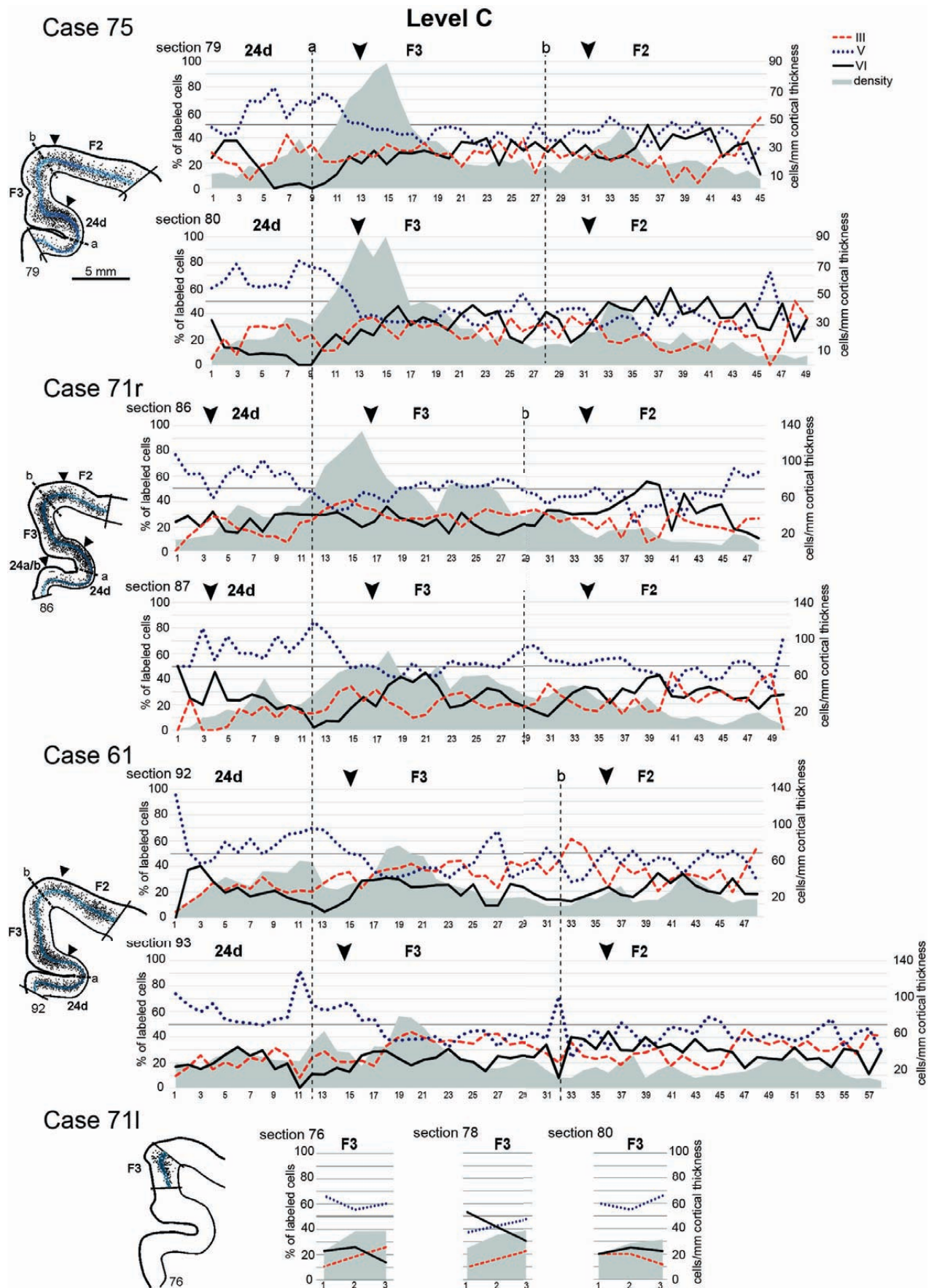


Case 71r

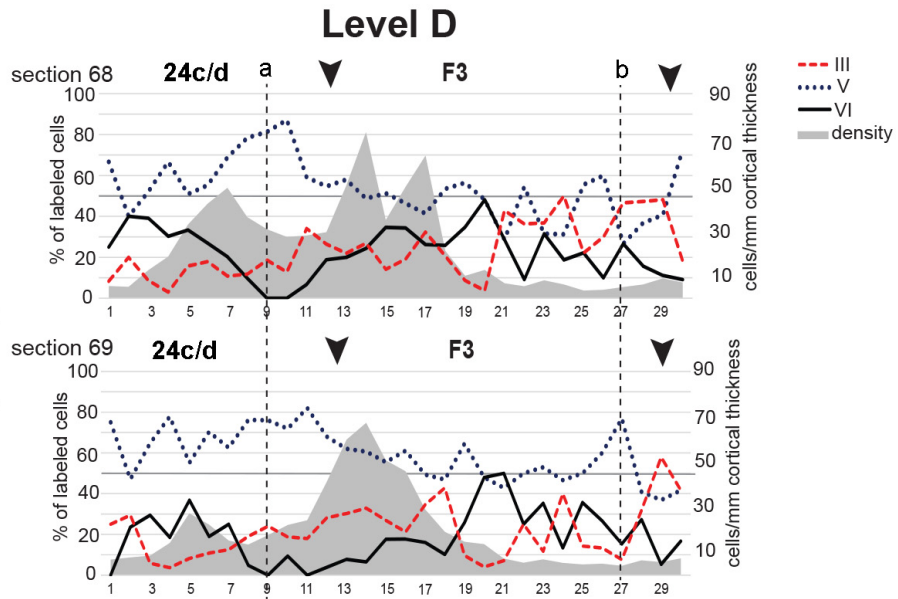
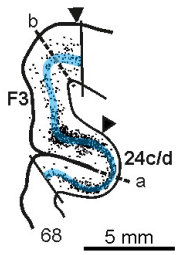


Case 61

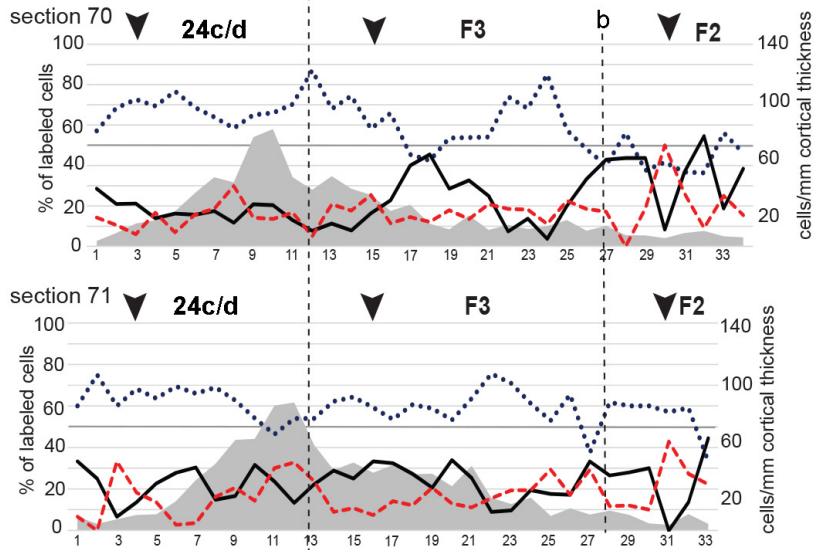
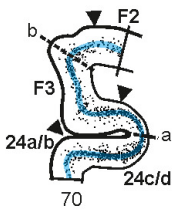




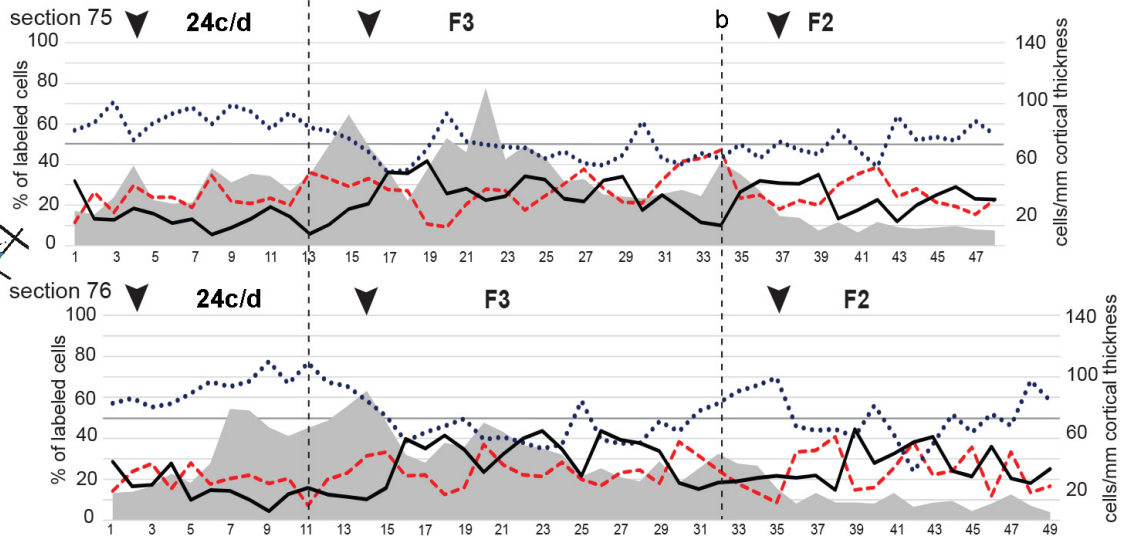
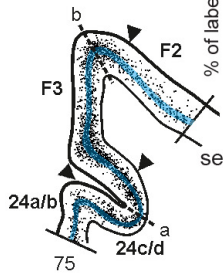
Case 75

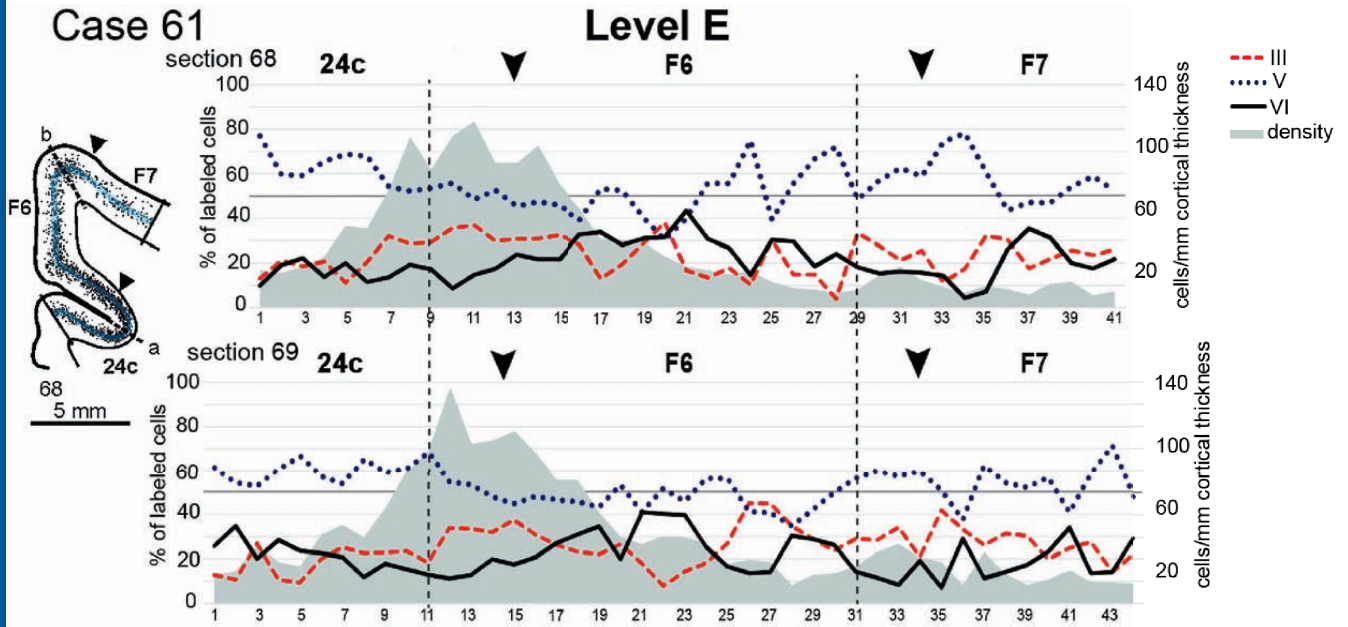


Case 71r



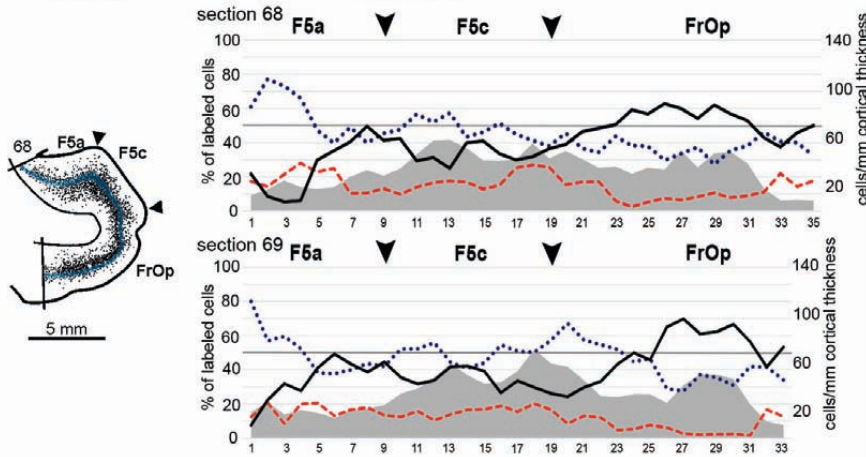
Case 61





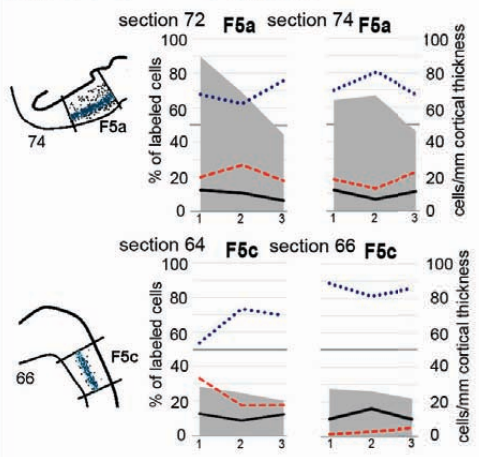
Case 61

Level E



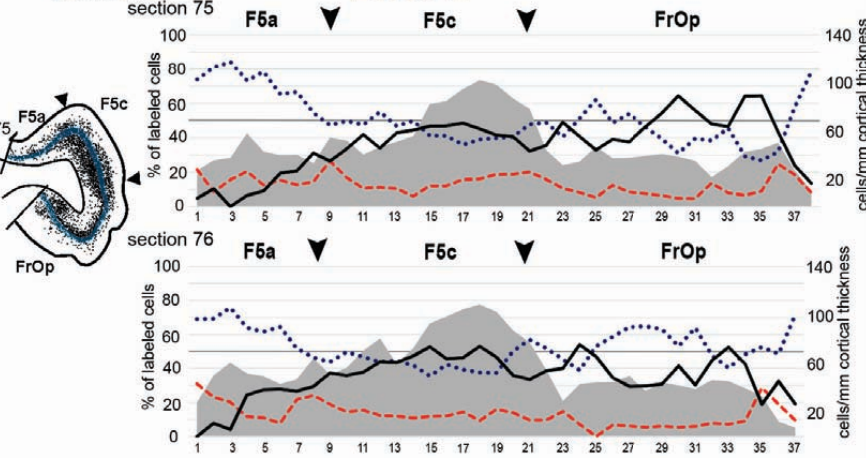
Case 71l

Level D



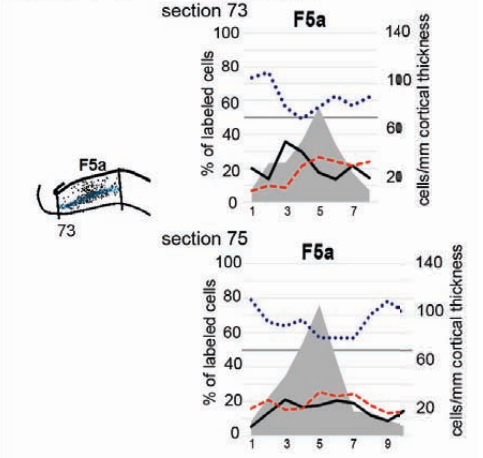
Case 61

Level D



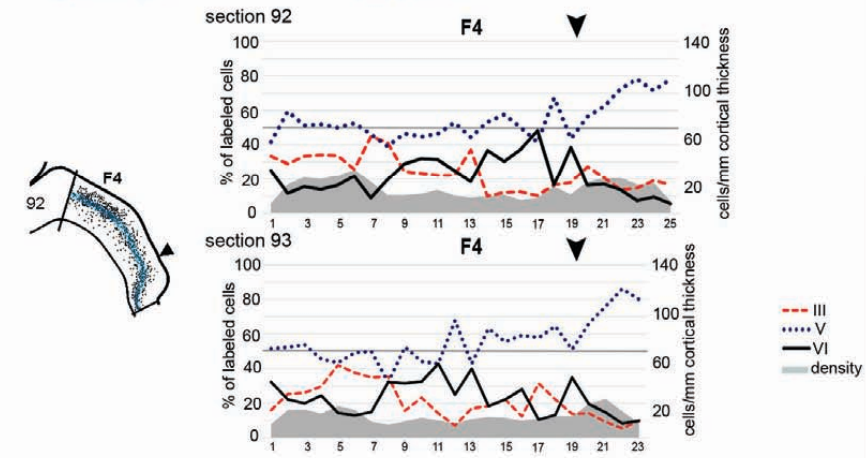
Case 71r

Level D



Case 61

Level C



Case 71r

Level C

